Journal of Medicinal Chemistry

pubs.acs.org/jmc

Article

Bispecific Estrogen Receptor α Degraders Incorporating Novel Binders Identified Using DNA-Encoded Chemical Library Screening

Jeremy S. Disch,* Jennifer M. Duffy, Esther C. Y. Lee, Diana Gikunju, Betty Chan, Benjamin Levin, Michael I. Monteiro, Sarah A. Talcott, Anthony C. Lau, Fei Zhou, Anton Kozhushnyan, Neil E. Westlund, Patrick B. Mullins, Yan Yu, Moritz von Rechenberg, Junyi Zhang, Yelena A. Arnautova, Yanbin Liu, Ying Zhang, Andrew J. McRiner, Anthony D. Keefe, Anna Kohlmann, Matthew A. Clark, John W. Cuozzo, Christelle Huguet, and Shilpi Arora*

Cite This: J. Med. Chem. 2021, 64, 5049−5066

Read Online

ACCESS | Metrics & More | Article Recommendations | Supporting Information

ABSTRACT: Bispecific degraders (PROTACs) of ERα are expected to be advantageous over current inhibitors of ERα signaling (aromatase inhibitors/SERMs/SERDs) used to treat ER+ breast cancer. Information from DNA-encoded chemical library (DECL) screening provides a method to identify novel PROTAC binding features as the linker positioning, and binding elements are determined directly from the screen. After screening ∼120 billion DNA-encoded molecules with ERα WT and 3 gain-of-function (GOF) mutants, with and without estradiol to identify features that enrich ERα competitively, the off-DNA synthesized small molecule exemplar **7** exhibited nanomolar ERα binding, antagonism, and degradation. Click chemistry synthesis on an alkyne E3 ligase engagers panel and an azide variant of **7** rapidly generated bispecific nanomolar degraders of ERα, with PROTACs **18** and **21** inhibiting ER+ MCF7 tumor growth in a mouse xenograft model of breast cancer. This study validates this approach toward identifying novel bispecific degrader leads from DECL screening with minimal optimization.

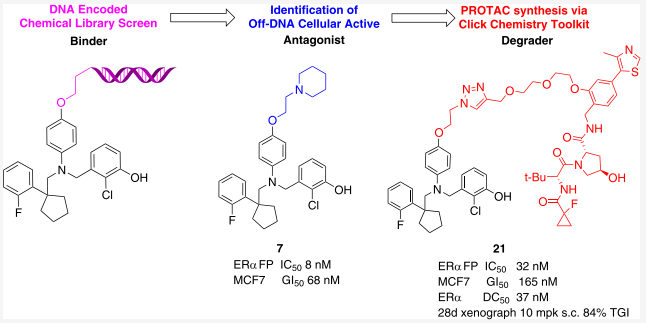

INTRODUCTION

Breast cancer is the most common cancer in women, with an annual worldwide incidence of ∼2 million and accounting for 15% of all cancer-related deaths in women.[1] Estrogen receptor (ER) is a ligand-dependent nuclear hormone receptor, which, upon activation, acts as a transcription factor in normal breast cells. ERα, one of the two main subtypes of estrogen receptor, is over-expressed in ∼70% of all breast cancers. ERα signaling is responsible for cancer cell proliferation, survival, and metastasis in breast cancer.[2] Approved endocrine therapies include aromatase inhibitors (AIs) such as letrozole, selective ER modulators (SERMs) such as tamoxifen, and selective ER degrader (SERDs) such as Fulvestrant. These therapies have allowed for effective management of ER+ breast cancer.[3] Fulvestrant's approval as a first line therapy for metastatic ER+ breast cancer suggests that degradation of estrogen receptor is a valid and useful strategy for treating breast cancer.[4] Poor pharmacokinetic properties of Fulvestrant have inspired the development of second generation SERDs, both steroidal and non-steroidal, that are currently in clinical trials or under development. These include compounds in Phase 2/3 clinical trials, Elacestrant (Radius), RG6171 (Roche), SAR439839 (Sanofi), and AZD9833 (AstraZeneca), and others in Phase 1 from Eli Lilly, Novartis, G1 Therapeutics, and Pfizer.[4−7] For currently approved therapeutics, despite initial efficacy, the development of acquired resistance limits their utility. Gain-of-function (GOF) mutations in ERα are enriched in one-third of endocrine therapy-resistant recurrences, leading to ligand-independent activation of the ERα pathway,[8,9] thereby conferring partial resistance to existing classes of endocrine therapies. These acquired mutations are associated with aggressive disease biology and reduced overall survival.[10] The most common among these GOF mutations result in altering the amino acids Y537 and D538, generating a constitutively active ER.[11−13] These GOF mutants are resistant to estrogen deprivation and are less responsive to tamoxifen or Fulvestrant. Thus, there is a need to develop a next generation of ERα-targeted therapeutics that can address aberrant activities of both wild-type and GOF mutants of ERα.

Received: January 22, 2021
Published: April 12, 2021

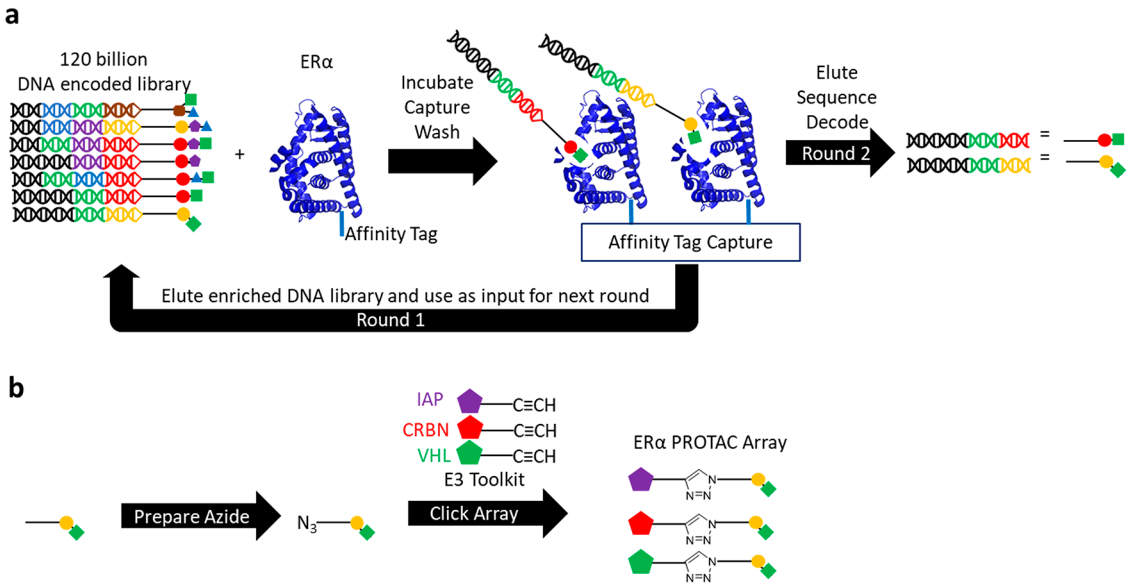

Figure 1. Schematic for DECL screening and PROTAC array platforms. (a) DNA-encoded chemical library (combinatorial synthesized small molecules tethered to DNA tags) is incubated with ERα, affinity captured, washed to remove non-binding library, and then enriched library members are eluted. After repeating an additional round, the DNA tags are sequenced to identify the small molecule binders. (b) Azide variants of the binders are prepared and reacted in a parallel click chemistry library of E3 binder alkynes to obtain an array of PROTACs for ERα.

Recently, bispecific degraders (PROTACs, proteolysis targeting chimeras) have emerged as a novel therapeutic strategy in drug discovery and development and the first PROTAC compounds have recently entered into clinical trials.[14,15] These bispecific degraders utilize two active domains attached with a linker, allowing for the protein of interest (POI) to be held in close proximity to a targeted E3 ligase, thus targeting the former for degradation through the ubiquitin proteasome system.[16,17] Most ERα-targeting bifunctional degraders are based on well-known binders to ERα, such as raloxifene, tamoxifene, lasofoxifene, or estradiol, among others.[4,18−23] Though an immensely promising technology, the field acknowledges issues with optimization of these molecules, such as linker presentation, which may be a limiting factor in optimal design. However, one of the biggest challenges is identifying novel POI and ubiquitin ligase binders.[24] The necessity for a tether may be best approached using screening methodologies that utilize tethered molecules. Thus, an approach like DNA-encoded chemical libraries (DECL) screening may be the best option for identifying such novel ligands.

Herein, we report the discovery of a series of novel ERα bispecific degraders (PROTACs) that target both WT and mutant ERα, by utilizing DECL screening to discover novel ERα binders and antagonists, and quickly using this information to develop novel POI engagers for generating bifunctional degraders. DECL platforms have emerged as an attractive approach to affinity screen billions of compounds in a single selection experiment.[25] This platform uses split and pool combinatorial chemistry to synthesize very large, thousands to billions, member combinatorial libraries, in which a unique DNA sequence is covalently tethered to each small molecule. The DNA sequence is used to record the library, building block, and reaction information during the course of library synthesis. DECL technology has generated several clinical candidates[2627−28] and, most recently, has been extended to screens in live cells[29] and used to train machine learning models.[30]

In a typical DECL screening campaign (Figure 1a), DNA-encoded libraries are incubated with a protein, affinity captured, and washed to enrich the library pool. The final selection output is amplified, sequenced, and translated to identify the structures of the tethered small molecules. DECL selections are frequently multiplexed, allowing for comparative evaluation of enrichment to define a mechanism of action. For instance, by screening homologs or including a known competitor, substrate, or cofactor during the selection process, one can focus on a particular binding profile, mutant, or species specificity.[25,29] Once the structures are translated from the DNA tag sequences, structures are filtered by removing promiscuous and matrix binders. After evaluating the enrichment profile across the multiplexed selection conditions, hits are synthesized off-DNA to confirm binding in assays.

A key advantage of the DECL platform is that a substantially large collection of novel tethered molecules is being presented to the target in their linked presentation, a key requirement for the development of PROTACs. After identification of a valid binder to a protein of interest, the DECL information can be directly leveraged to produce PROTACs very efficiently by preparing an azide linked variant with the DNA tag replaced by an azide and then cross-reacted with a series of E3 binder alkynes utilizing click chemistry[31] (Figure 1b). Ultimately, this would lead to sets of PROTACs, with novel POI binders identified by large combinatorial space to progress into biochemistry, cellular biology, ADME, and efficacy studies.

RESULTS

Affinity-Mediated Selection of DNA-Encoded Chemical Libraries. To identify novel ERα binders, we conducted a DNA chemical library affinity screen utilizing X-Chem's ~120-billion-member library collection. A collection of 44 distinct DNA-encoded chemical libraries were combined and incubated with no target, the ligand binding domains (LBD) of ERα WT 7.7 μM to 24 nM, ERα WT at 7.7 μM with estradiol at 15 μM, and each of three mutant forms of ERα, D538G, S463P, and Y537S at 7.7 μM. Supplementary Figure S1 shows

https://doi.org/10.1021/acs.jmedchem.1c00127
J. Med. Chem. 2021, 64, 5049−5066

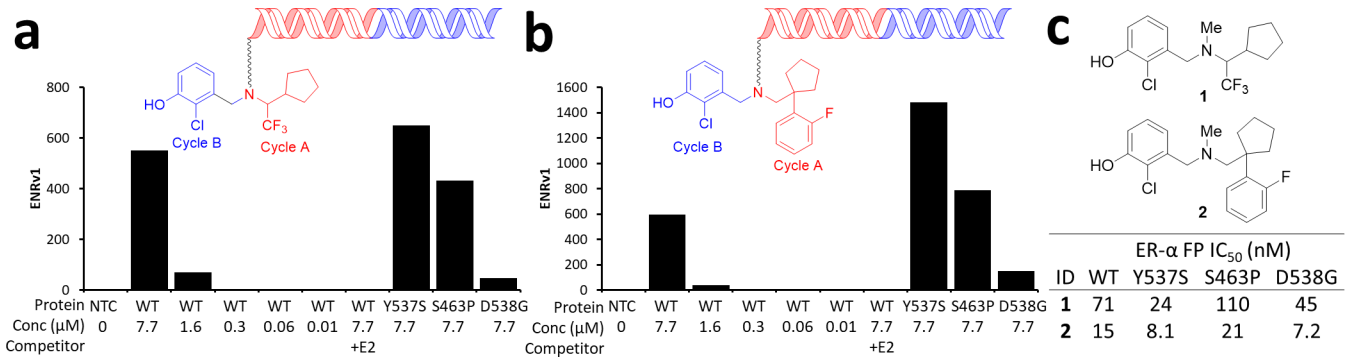

Figure 2. DECL selection output and off-DNA activity confirmation of two related members. (a, b) Schematic of two structurally related 2-cycle library members and their enrichment (ENRv1) suggests they bind ERα WT and mutants Y537S, S463P, and D538G. These library members do not bind the matrix (NTC; no target control) and are competed off by the presence of Estradiol (E2), suggesting that these library members bind in the ligand binding site. (c) Analogous "off-DNA" synthesized exemplars, with the linker and DNA truncated to a single methyl, bind in fluorescence polarization binding displacement assay. Assay results are an average of duplicate runs.

a denaturing PAGE of all the ERα LBD variants used in the affinity-mediated selection with the DNA-encoded chemical libraries. Proteins and associated library members were captured using an IMAC matrix followed by stringent washing and elution at 85 °C. The output of the first round of selection was used as the input for the second round of selection with fresh protein and competitor reagents, and the output of the second round of selection was PCR-amplified and submitted for Illumina sequencing. A total of 528 million single-end reads were generated across all 44 libraries, and all selection conditions averaged 1.2 million reads per library per selection condition.

Selection Output Data Analysis and Hit ID. Individual sequence reads were translated back into the corresponding building block, and library schemes and statistical prevalence data were calculated for all building block combinations in each library across all selection conditions. A large number of strongly enriched building block combinations were observed across all libraries. During the process of deciding which compounds to synthesize off-DNA for hit-confirmation, a range of parameters was considered including the extent of enrichment, the profile of enrichment across the different protein variants, whether competition was observed with estradiol, how the enrichment extent varied across the dilution series, and the extent to which "SAR" was observed for co-enriching building blocks that manifest themselves in structurally related compounds. Enrichment profiles were calculated for each building block combination and the extent to which individual building block combinations co-enriched. Data are presented in Figure 2a,b for two individual building block pairs (disynthons) that were resynthesized off-DNA, determined to be active, and then used as the founder members or hits to establish the series. The relative enrichment of the two representative building block pairs can be seen across the selection conditions with each showing significant enrichment at 7.7 and 1.6 μM ERα, competition with estradiol, and also significant enrichment against the Y537S and S463P mutants with lesser enrichment against the D538G mutant. ENRv1 represents a statistical metric of enrichment significance for each disynthon (negative log10 of the asymptotic significance value).[32]

Hit Confirmation and SAR Follow-Up. To confirm the selection output, direct representative off-DNA compounds were synthesized, and their biochemical and cellular activities were evaluated. Two of the most potent off-DNA representative compounds (**1** and **2**) identified in the screen are shown in Figure 2c. The potency of these ERα binders was assessed in an *in vitro* biochemical FP (fluorescence polarization) assay that was established for ERα WT and three of the most commonly occurring mutants, S463P, Y537S, and D538G. Compounds identified to be active in the biochemical assay were then tested in a dose titration in the ER+ cell line, MCF7, in a proliferation assay in both antagonist and agonist mode.[33] The preferred phenotype in the cell-based assay is an anti-proliferative effect on ER-dependent cells in antagonist mode (+E2), with no increase in growth of cells seen in hormone-deprived media (agonist mode).[33] In addition to the proliferation assay, PROTACs were also tested in an ERα degradation assay in MCF7 cells (in-cell western assay) to confirm the degradation of ERα in cells. ERα levels were assessed in dose titration upon 24 or 48 h exposure to the respective compounds.[33]

The chlorophenol compounds (**1** and **2**) were potent binders of WT and mutant (S463P, Y537S, and D538G) ERα LBDs with **2** having 2- to 5-fold higher potency than **1** (Figure 2c), and both had modest cellular agonist activity (0.46−0.55 μM) in MCF7 cells (Table 1). With the guidance of the DECL screening selection data and molecular docking, we designed, prepared, and evaluated the *in vitro* small molecule SAR with an emphasis on potency and antagonism. The DNA-encoded library information indicated that the likely solvent accessible exit vector was at the tertiary amine that provides the connection between the encoded compounds and the linker to DNA. However, docking also suggested other poses with the fluorophenyl ring projecting toward solvent, with the phenol also buried deep in the pocket. We sought an approach to build SAR by maintaining potency while modulating the cellular activity from agonism to antagonism by appending a polar amine group off these vectors to interact with Asp351, which is known to introduce antagonism (see Table 1). Initially replacing the methyl with phenyl at R_1 gave compound **3**, which maintained binding activity (15 nM); however, this change resulted in producing a more potent cellular agonist (**3**, GI_{50} < 5 nM). Progressively longer alkyl-piperidine chains **4**−**7** correlated with improvements in potency, with **7** having the desired characteristics of notably potent antagonism, no observed cellular agonism, and interestingly, degradation of ERα as a small molecule in an in-cell western assay (DC_{50} = 15

https://doi.org/10.1021/acs.jmedchem.1c00127
J. Med. Chem. 2021, 64, 5049−5066

Table 1. Off-DNA Small Molecule SAR[a]

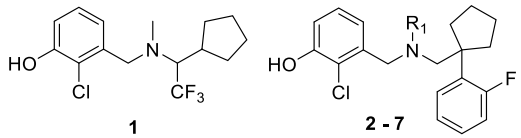

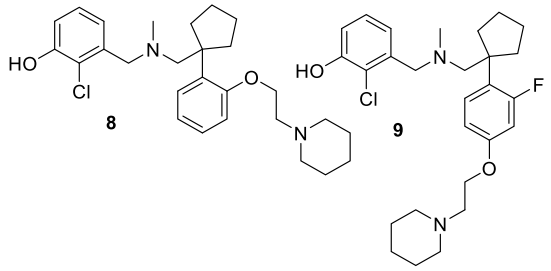

		ER-α FP IC_{50} (μM)	MCF7 GI_{50} (μM)	
ID	R_1	WT	Agonist	Antagonist
1		0.071	0.46	>10
2	-Me	0.015	0.55	>10
3	-Ph	0.015	<0.005	>10
4		>10	ND	ND
5	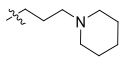	0.96	ND	ND
6	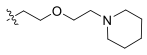	0.083	>10	3.1
7	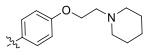	0.008	>10	0.068
8		>10	>10	3.14
9		0.062	<0.005	>10

[a]The structure−activity relationships for small molecules without DNA barcodes in ERα binding FP assay, MCF7 agonism and antagonism viability, and ERα degradation (DC_{50}). ND = not determined. Results in the table represent an average of duplicate runs.

nM; $D_{max} \approx 70\%$) in starved CSS media conditions. Curiously, the other attachment points appeared to generate a significantly weaker binder (**8**) or potent agonist behavior (**9**), indicating that there was sensitivity to the linker location. We decided to further progress compound **7** forward as a moiety in a bispecific PROTAC format.

Development of Potent ERα Binders into PROTACs. To determine if our internal PROTAC strategy was feasible, we started with a known ERα binder, bazedoxifene,[34,35] to rapidly identify which E3 ligands could be utilized to degrade ERα protein. To concurrently explore the effect of different E3 targeting ligands and linker lengths for attaching the ERα binding moiety, we utilized an exploration strategy that capitalizes on Huisgen 1,3-dipolar cycloaddition reaction. Commonly referred to as "click chemistry," the cycloaddition forms a triazole ring by reacting an azide and an alkyne moiety under relatively mild conditions (Table 2). A toolbox of E3 ligase binders with varying linker lengths to alkynes[31] enabled the parallel synthesis of PROTACs with the azide of a POI binder in a facile manner. Our toolbox included alkynes linked to cereblon, VHL, and IAP E3 ligase binders with one, two, or three PEG units between the E3 binder and the azide moiety (Table 2).

From the literature, it is known that the indole portion of bazedoxifene binds to the ligand-binding domain of the estrogen receptor and thus the azepane points toward the solvent.[34] Therefore, an azide version of bazedoxifene was prepared to react with the corresponding E3 binder alkynes to produce PROTACs based on thalidomide (**10**); VHL amide (**11**−**13**), VHL-phenoxy (**14**), IAP phenoxy (**15**), and IAP amide (**16**). These compounds were tested in a binding assay as well as the previously described cellular degradation and viability assays. All seven compounds were potent in the binding assay (Table 2, IC_{50} range 1.6−52 nM). However, only the VHL amide (**11**−**13**), VHL phenoxy (**14**), and IAP phenoxy (**15**)-based PROTACs had sub-micromolar cellular degradation. These same compounds were also confirmed to be antagonists in the cellular viability assay with GI_{50} values ranging from 34 to 335 nM (Table 2), demonstrating that VHL-based PROTACs with bazedoxifene generate potent degraders (**11**−**14**).

Based on the success of utilizing a VHL engager in the proof of concept bazedoxifene series, we decided to focus on the VHL ligands for designing PROTACs with our structurally novel series. Click chemistry on an azide intermediate of **7**, where an azide replaced the piperidine in compound **7**, was used to prepare an array with three linker length alkynes of PROTACs based on VHL amide (**17**−**19**) and VHL-phenoxy (**20**−**22**). The binding affinity of the VHL amide PROTACs **17**−**19** seemed less potent with increasing linker length (2- to 5-fold). However, the cellular degradation potency values (DC_{50}) for all three PROTACs were single-digit nM. In the VHL phenoxy series, the binding affinities of **21** and **22** were similar (IC_{50} = 32 and 44 nM), whereas the shortest linker **20** was less potent (IC_{50} = 198 nM). Unpredictably, the cellular ERα degradation of **20** and **21** was the same (38 and 37 nM), and the compound with the longest linker **22** was more potent and with similar potency to the VHL amides at 5.3 nM (Table 2). These compounds were also tested in the corresponding binding assay with mutants D538G, S463P, and Y537S and showed pan inhibition with binding within 20-fold of WT. All compounds were shown to be antagonists in the cell viability assay (Table 2).

Understanding the MOA and Kinetics of ERα Inhibition and Degradation in MCF7 Cells. Two of the most potent PROTACs from the two VHL variants (**18** and **21**) were utilized to understand the mechanism of action (MOA) of ERα inhibition and degradation (structures shown in Figure 3a). Biochemically, both compounds were very potent in the WT and mutant ERα FP binding assays (Figure 3b and Table 2). In-cell western-based degradation assay in MCF7 cells showed dose-dependent reduction in the levels of ERα at 24 h, with both compounds tested, **18** (DC_{50}: 4.5 nM) and **21** (DC_{50}: 20 nM; Figure 3c and Supplementary Figure S2). These graphs represent normalized ERα levels. We did not assess D_{max} as a parameter in this study (due to the use of a

https://doi.org/10.1021/acs.jmedchem.1c00127
J. Med. Chem. 2021, 64, 5049−5066

Table 2. PROTACs Utilizing a Bazedoxifene or Compound 7 Moeity as the POI Binder[f]

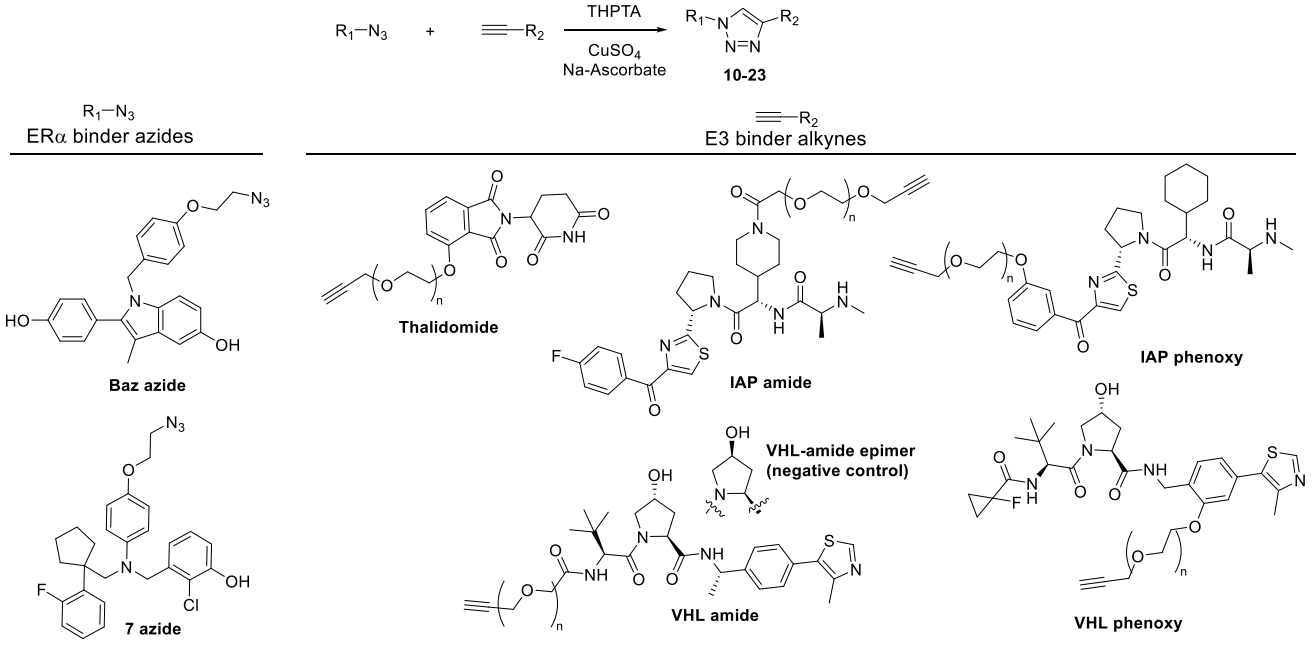

	PROTAC made from:			ERα FP IC_{50} (nM)				MCF7 GI_{50} (μM)		MCF7 DC_{50} (μM)
ID	ERα binder azide	E3 binder alkyne	*n*	WT	S463P	Y537S	D538G	Ag.	Ant.	degradation
10	Baz azide	Thalidomide	1	1.6	2.1	3.2	4.7	>10	3.25	2.5[a]
11	Baz azide	VHL amide	1	11	21	8.1	287	>10	0.247	0.020[a]
12	Baz azide	VHL amide	2	22	18	38	27	>10	0.335	0.020[a]
13	Baz azide	VHL amide	3	22	6.0	15	9.3	>10	0.211	0.009[a]
14	Baz azide	VHL phenoxy	1	5.3	14	52	29	>10	0.034	0.027[b]
15	Baz azide	IAP phenoxy	1	7.3	24	61	40	>10	0.051	0.174[b]
16	Baz azide	IAP amide	1	52	ND	ND	ND	>10	>10	>10[c]
17	7 azide	VHL amide	1	17	170	332	269	>10	0.165	0.0042[b]
18	7 azide	VHL amide	2	53	203	419	517	>10	0.030	0.006[b]
19	7 azide	VHL amide	3	97	238	534	332	>10	0.261	0.008[b]
20	7 azide	VHL phenoxy	1	198	1129	3720	2205	>10	0.423	0.038[b]
21	7 azide	VHL phenoxy	2	32	143	527	329	>10	0.165	0.037[b]
22	7 azide	VHL phenoxy	3	44	134	302	261	>10	0.131	0.0053[b]
23	7 azide	VHL amide epimer	2	90	122	341	199	>10	1.75	1.78[b], >10[d,e]

[a]Original assay. [b]48 h. [c]24 h. [d]6 h. [e]16 h. [f]Individual compounds from the PROTAC array design were prepared utilizing click chemistry to obtain PROTACs **10**–**23** with variable ERα and E3 binding elements and variable linker lengths (*n*). The compounds were assessed in FP binding assays for WT and mutant ERα, MCF7 viability assay in agonist or antagonist mode, and in MCF7 in cell western ERα degradation. ND = not determined. Results in the table represent an average of duplicate runs.

PROTAC control rather than an absolute control in the assay), but upon comparing the two compounds, we saw at least 20% more degradation of ERα with **21** than **18**, demonstrating a more robust degradation for **21**. Next, the cellular viability assay in MCF7 cells demonstrated negligible agonist effects, while both compounds demonstrated robust antagonistic activity (Figure 3d). As ERα is a transcription factor, we next tested its immediate downstream effect on the gene expression of its target progesterone receptor (PGR). The results demonstrated a dose-dependent reduction in the levels of PGR upon treatment with **18** (EC_{50} 27 nM) and **21** (EC_{50} 90 nM) at 24 h (Figure 3e). The graphs represent normalized PGR levels.

In order to assess the kinetics of PROTAC-mediated ERα degradation, we performed time-course experiments followed by western blotting to determine optimal ERα degradation with PROTACs in both hormone-deprived media (agonist mode) and full-serum media (antagonist mode). MCF7 cells were treated with 1 μM Fulvestrant or **18** over a time course of 48 h. Results demonstrated degradation of ERα with Fulvestrant 4 h after treatment, but complete degradation with Fulvestrant under these conditions was not observed (Figure 4a). In contrast, strong, near-complete degradation was seen as early as 2 h with PROTAC-based degrader **18** (Figure 4a) (data for agonist mode not shown but was similar to antagonist mode). Next, to understand the durability of ERα degradation, we performed a wash-out experiment. Upon compound wash-out, we observed a 10-fold loss in degradation efficacy with **18**, but **21** demonstrated a 25-fold reduction (Figure 4b). In order to confirm that the observed degradation is VHL-mediated, we performed a competition experiment utilizing the E3 binder, VHL-298 (Figure 4e).[36] Cells co-treated with VHL-298 (5 μM) alongside ERα PROTACs (**18** or **21**) observed a DC_{50} shift of ∼8-fold, supporting the hypothesis that VHL-engagement is required for proteasome-mediated degradation of ERα (Figure 4c).

https://doi.org/10.1021/acs.jmedchem.1c00127
J. Med. Chem. 2021, 64, 5049−5066

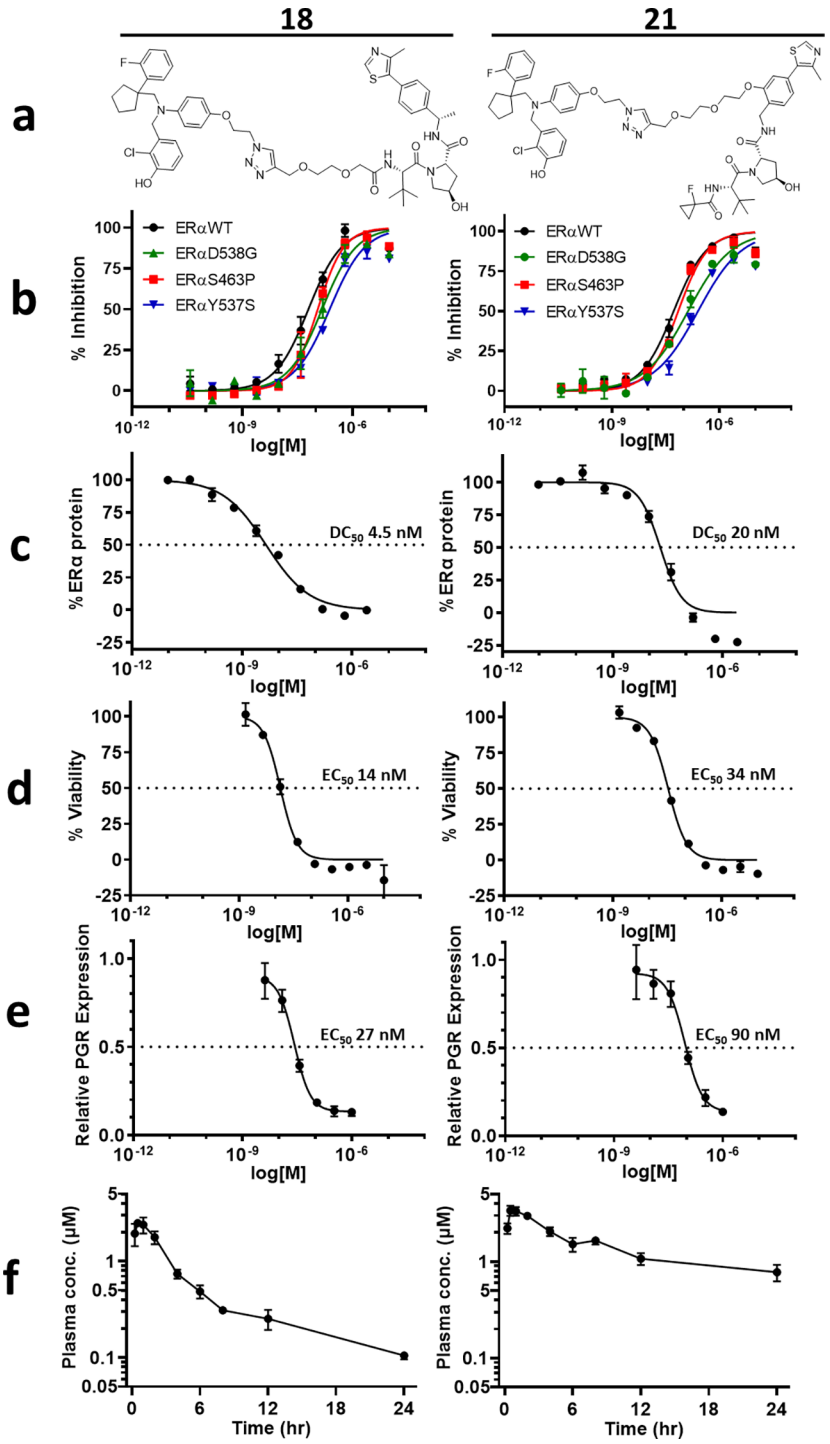

Figure 3. Biochemical, cellular, and mouse PK properties of ERα PROTACs, **18** and **21**. (a) Structures of **18** and **21**. (b) Biochemical inhibition using purified recombinant ERα WT and mutants D538G, Y537Y, and S463P. (c) Degradation of ERα in MCF7 cells treated for 24 h followed by in-cell western analysis of ERα protein normalized to tubulin. The graphs represent normalized ERα levels. (d) MCF7 viability assay with cells treated for 7 days followed by an end-point viability by CellTiter-Glo. (e) Downstream PGR expression analysis in MCF7 cells treated for 24 h followed by RNA extraction, first strand synthesis, and qPCR analysis for progesterone receptor RNA estimation, normalized to TBP (Tata-binding protein); graphs represent normalized PGR levels. (f) Mean plasma concentration (μM) for 10 mpk (mg/kg) subcutaneous dosing in CD1 mouse (n = 3). Curves shown are from a single run with technical replicates.

To additionally confirm the PROTAC mechanism is working *via* VHL engagement, we prepared the VHL prolinol epimer **23** of compound **18** as a negative control. Although the ERα binding potency for the negative control VHL amide epimer **23** was 90 nM, the in-cell western degradation result at 48 h showed markedly less potent degradation (>770-fold) than the corresponding active degrader **18** (Figure 4d). To further explore the ameliorated activity of compound **23**, we also evaluated the degradation at shorter timepoints (6 and 16 h) to reduce any potential assay interference/toxicity. At these shorter timepoints, compound **23** exhibited no protein degradation. Therefore, we concluded that, at longer time-

https://doi.org/10.1021/acs.jmedchem.1c00127
J. Med. Chem. 2021, 64, 5049−5066

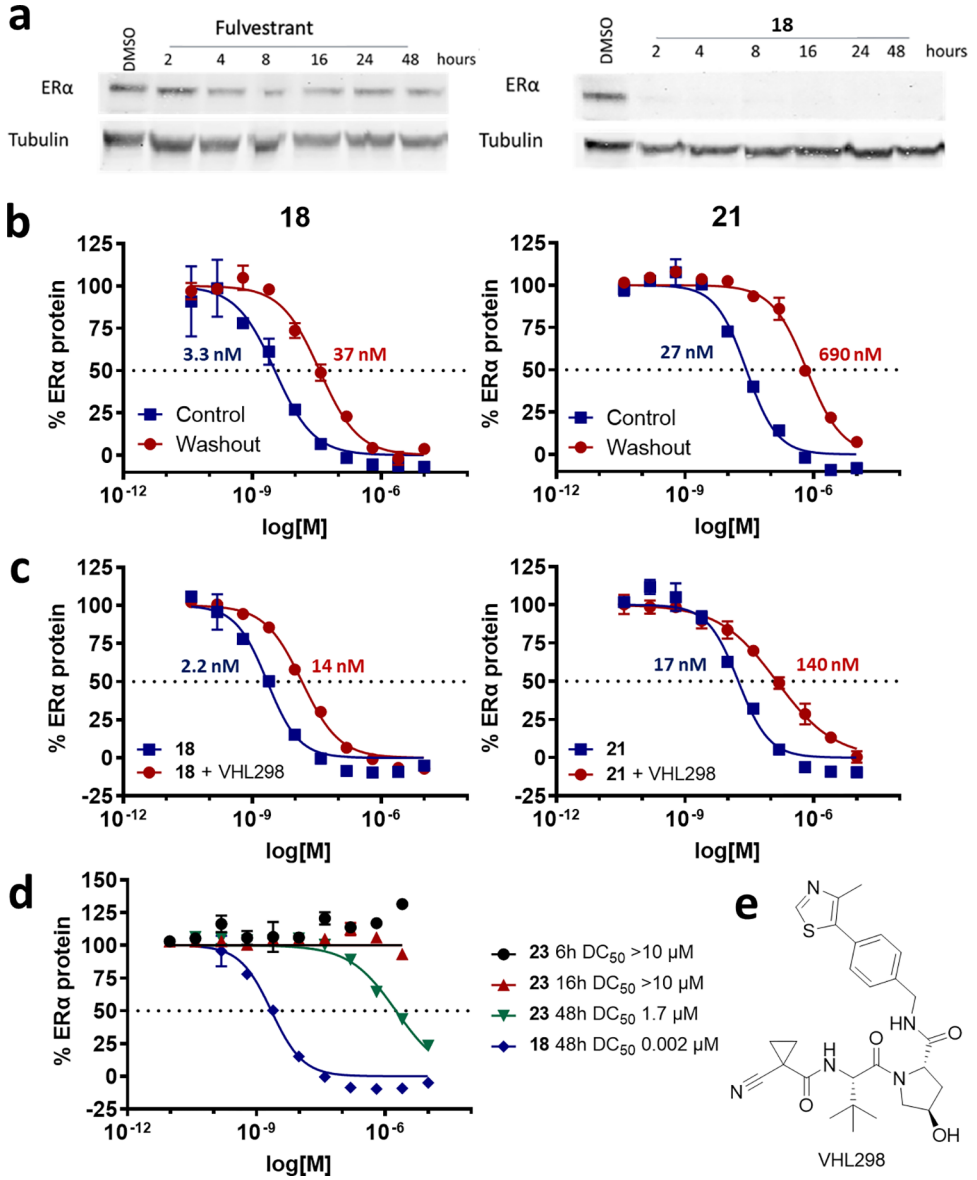

Figure 4. ERα PROTACs inhibit and degrade ERα in MCF7 cells. (a) Time course degradation of ERα treated with Fulvestrant (1 μM) or **18** (1 μM). Cells were lysed and assayed by western blot, and tubulin was used as a normalizer control. (b) In-cell western evaluating the persistence of degradation effect after a 2 h treatment, compound washout and cell collection after another 22 h, compared to full 24 h compound treatment. Continued ERα reduction was observed after the washout. ERα normalized to tubulin control. (c) Proteasomal degradation of ERα is VHL-mediated by observing that co-treating with VHL298 (5 μM, literature K_d = 90 nM) resulted in a higher DC_{50} compared to compound alone, 48 h total treatment time followed by collection. (d) Degradation of ERα is significantly impaired in the negative control prolinol epimer **23** compared to the analogous active prolinol epimer **18**, showing that degradation is proceeding through a VHL-based mechanism. (e) Structure of VHL298. All traces and DC_{50} values are from a single experiment with technical replicates.

points (48 h), the slight reduction in protein levels was likely due to compound toxicity, and the degradation of ERα of this novel series proceeds through VHL-mediated degradation.

PROTACs Degrade ERα in Multiple ER-Positive Cell Lines and Reduce Cell Viability. To demonstrate degradation of ERα across multiple cell lines, we tested ERα PROTACs, **18** and **21**, in an additional ER-positive cell line, T47D. MCF7 and T47D cell lines were treated with increasing doses of **18** and **21** for 24 h. Cell lysates were prepared, and western blotting was performed, with Actin used as a loading control. Similar to observations with the MCF7 cell line, robust ERα degradation was observed in T47D cells and the DC_{50} values for the two cell lines were very similar (Figure 5a and Supplementary Figure S3). Given the remarkable potency of the compounds on all the GOF mutants, we would expect those ERα mutant proteins to be degraded in the cells, but due to unavailability of any commercially available cellular models for these mutants, we did not test this.

Next, to test on-target *vs* off-target effects, we tested various breast cancer cell lines; ER+ (MCF7, T47D, and ZR-75-1), ER-negative (MDA-MB-231), and an immortalized normal breast cell line (MCF10A) in cellular viability assays. Various breast cell lines were treated with increasing doses of ERα PROTACs, **18** and **21**, in full serum conditions for 7 days. Relative cell numbers were assessed using CellTiter-Glo.

As expected, the results showed viability defects in all ER+ cell lines with GI_{50} values ranging between 13 and 170 nM for **18** and 34 and 154 nM for **21**, while no effect on viability was

https://doi.org/10.1021/acs.jmedchem.1c00127
J. Med. Chem. 2021, 64, 5049−5066

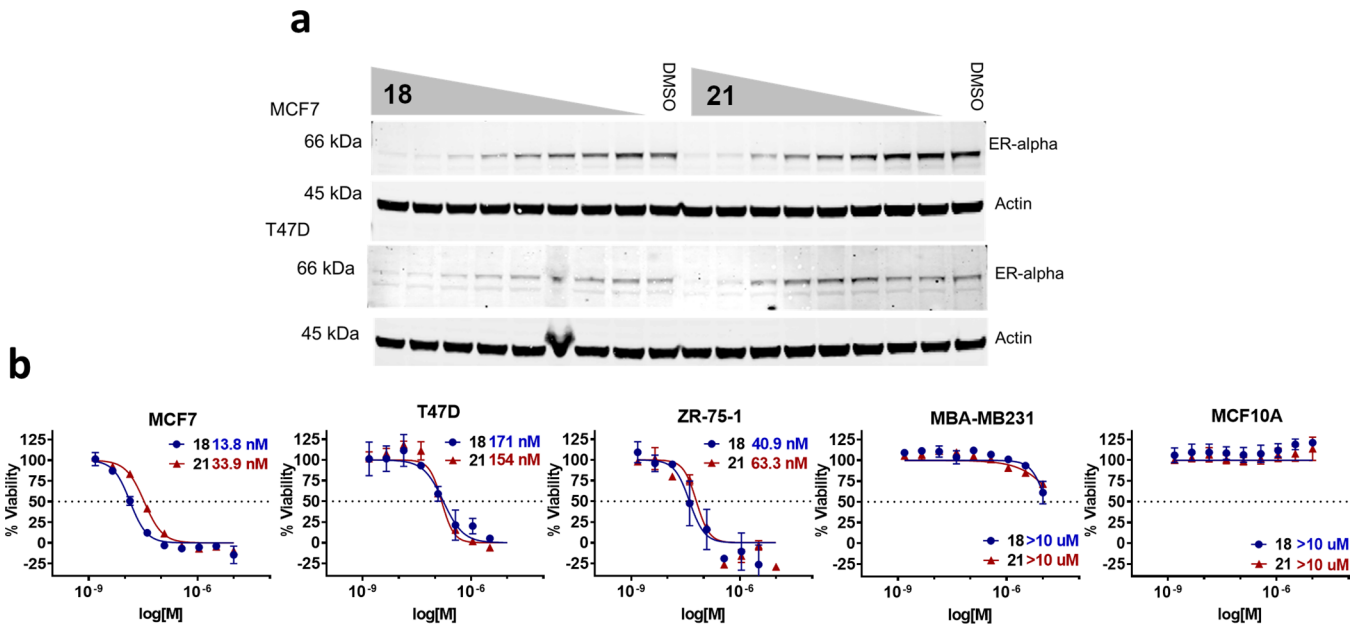

Figure 5. ERα PROTACs demonstrate on-target effects in ER+ cell lines and not in ER− cell lines. (a) MCF7 and T47D cell lines were treated with increasing doses of **18** and **21** for 24 h showing ERα degradation. Cell lysates were prepared and western blotted for ERα with Actin as a loading control. (B) ER-positive (MCF7, T47D, and ZR-75-1) and ER-negative breast cancer cell lines (MBA-MB231) and immortalized breast cell line (MCF10A) were treated with increasing doses of ERα PROTACs, **18** and **21**, in full serum conditions for 7 days. Relative cell numbers were assessed using CellTiter-Glo.

Table 3. *In Vitro* Clearance and *In Vivo* PK of Select Compounds in Male CD1 Mice[a]

	microsomal stability		i.v. PK CD1 mouse			s.c. PK CD1 mouse			
ID	HLM CL_{int} (μL/min/mg)	MLM CL_{int} (μL/min/mg)	Cl_{obs} (mL/min/kg)	$Vd_{ss,obs}$ (L/kg)	$T_{1/2}$ (h)	C_{max} (μM)	AUC_{inf} (μM·hr)	$T_{1/2}$ (h)	%F
17	31	199	20	1.24	2.7	1.50	9.8	21	83
18	59	249	23	4.82	8.7	2.13	14.6	17	>100
20	42	162	1.2	0.12	2.2	2.08	44.5	21	20
21	47	139	0.9	0.18	4.7	3.55	53.9	17	25

[a]Human (HLM) and mouse (MLM) liver microsome stability. All compounds were formulated in 40% HP-β-CD in water. Cl_{obs}, Vd_{ss} $T_{1/2}$ determined by 0.3 mg/kg CD1 mouse IV dose cassette dosing, C_{max}, AUC_{inf}, and $T_{1/2}$ were determined by 10 mpk subcutaneous in CD1 mouse, % *F* is reported for AUC_{inf} (sc/iv).

seen in ER-negative breast cancer cell line MBA-MB 231 and the immortalized breast cell line MCF10A (Figure 5B). These results confirm the on-target effects of this new series of ERα PROTACs.

***In Vitro* ADME and PK.** Overall, the amide and phenoxy VHL-based compounds **17**−**22** were potent degraders of ERα in ER+ cell lines, and we sought to evaluate the series further *in vivo*. For both classes, we decided to progress the two shortest of the three linker lengths **17**, **18**, **20**, and **21** in *in vitro* ADME assays and in mouse intra-venous and subcutaneous PK studies (Table 3). In general, the optimization of ADME/PK of PROTACs can be challenging.[37] These compounds all have low solubility (<0.2 μM), low permeability (MDCK P_{app} A-B < 0.1 cm/s × 10^{-6}), and high PPB (>99.6%) (data not shown). These compounds do have moderate *in vitro* clearance in human and mouse microsomes (HLM CL_{int} = 31−59 mL/min/kg; MLM CL_{int} 139−249 mL/min/kg). *In vivo*, the IV clearance of the VHL phenoxy compounds **20** and **21** (CL_{obs} = 1.2 and 0.9 mL/min/kg) was much lower than the VHL amide **17** and **18** (20 and 23 mL/min/kg), and the volume of distribution is much lower for the VHL phenoxy linked PROTACs (**20**, **21**: Vd_{ss} = 0.12 and 0.18 L/kg) compared the VHL amide (**17**, **18**: Vd_{ss} =1.24 and 4.82 L/kg), resulting in higher exposures for VHL-phenoxy PROTACs (**20**, **21**: AUC_{inf} = 44.5 and 53.9 μM·hr) over VHL amide PROTACs (**17**, **18**: AUC_{inf} = 9.8 and 14.6 μM·hr), as seen in the exposure curve depicted in Figure 3f for **18** and **21**. Minimal exposure was observed when **18** and **21** were dosed orally (data not shown), which was anticipated given their low solubility and permeability, factors known to impede oral exposure.[38] Despite the low permeability, solubility, and high plasma protein binding of **18** and **21**, these two PROTACs present with potent degradation activity (though **21** leads to at least 20% greater D_{max} in cells), significant plasma exposures, yet differentiated PK profiles when dosed subcutaneously that warranted evaluation of ERα degradation in the *in vivo* setting.

***In Vivo* Efficacy Studies.** Based on reasonable subcutaneous single-dose PK data (10 mpk in CD1 mice) for **18** and **21** (Figure 3f) showing exposure over 24 h, we progressed these two lead PROTACs, **18** and **21**, into a mouse efficacy study. The MCF7 xenograft model was chosen, and we tested the two compounds alongside Fulvestrant (reference compound) in a 28 day efficacy study (8 mice/arm). Fulvestrant was highly effective in suppressing MCF7 tumor growth and on day 28, and TGI (tumor growth inhibition) of 91.6% was seen, $p < 0.001$. Subcutaneous administration of 10 mg/kg qd

https://doi.org/10.1021/acs.jmedchem.1c00127
J. Med. Chem. 2021, 64, 5049−5066

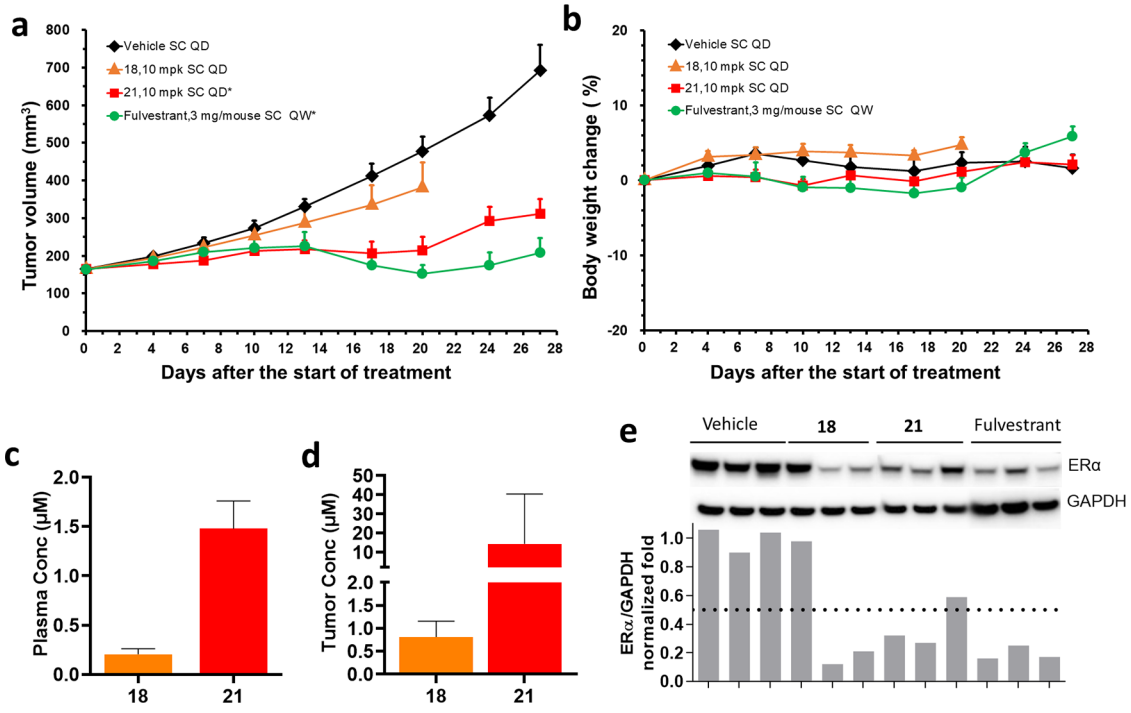

Figure 6. *In vivo* efficacy and PK/PD study demonstrating efficacy in MCF7 xenograft model. (a) Antitumor activity of **18** and **21** compared to Fulvestrant in WT Estrogen-dependent MCF7 xenograft model. **18** and **21** were administered subcutaneously once daily at 10 mg/kg. Fulvestrant was dosed SC QW at 3 mg/mouse. Data represent the mean tumor volume ± SEM ($n = 8$). *$p < 0.05$ versus vehicle control (Student's *t*-test). (b) All compounds were well tolerated with no changes in body weight. (c, d) Terminal Plasma PK and tumor PK of **18** and **21** at 3 h post-last dose (Day 20; **18**) and Day 27; **21**). (e) PD analysis from tumor bearing mice treated with compounds mentioned above for 3 days. Western blot analysis was performed to demonstrate reduction in ERα levels upon treatment with **18**, **21**, and Fulvestrant.

of **21** also demonstrated significant tumor growth inhibition (TGI) = 84.3%, $p < 0.001$. **18** at 10 mg/kg showed marginal effect on tumor volume (TGI = 30.8% $p > 0.05$), and as such, dosing was discontinued at day 20 (Figure 6a). No changes in average body weight in mice were recorded, and all compounds appeared to be well tolerated (Figure 6b). We collected plasma and tumor samples for end-point PK from the **18** and **21** arms, and the exposure in plasma and tumor correlated well with the efficacy seen *in vivo*, where **21** showed much better exposure as compared to **18** (Figure 6c,d), though high variability was observed in the levels of **21** measure in tumor samples at the end of the study. We also collected tumors from a separate set of mice treated with all three compounds for 3 days. Western blot results demonstrate a reduction in ERα levels in all treatment arms, though some mouse-to-mouse variability in the levels is observed (Figure 6e). These results clearly demonstrated that **21** is an excellent tool compound for inhibition and degradation of ERα both *in vitro* and *in vivo*.

DISCUSSION AND CONCLUSIONS

Since its introduction in 2001, the proteolysis targeting chimera (PROTAC) concept has been applied to many targets, including ERα.[18,19,39,40] Currently, there is one ERα PROTAC in the clinic[41] (ARV-471, structure was recently disclosed during review[23]), which is based on the cereblon binder lenalidomide and the SERM lasofoxifene. Although there are few other PROTACs in the clinic, the drug discovery path for PROTAC-based degraders is still being established, and there are many reviews trying to bring understanding to the community.[42−45] One of the challenges of discovering suitable PROTACs is finding an appropriate high affinity novel binder with a vector for attaching a linker to an E3 engager. DECL screening has a distinct advantage as an appropriate screening platform for designing PROTACs. Besides being an affinity (not activity)-based screening approach, the location of the linker attachment point is known *a priori*; thus, in the absence of structural information, the DNA-encoded chemistry platform affords a data-driven path forward to immediately begin linker optimization and small molecule bait presentation for a given POI. In conjunction with our DNA-encoded chemistry platform, we also established a toolkit to readily produce PROTACs based on well-known E3 ligase binders to enable the facile generation of arrays of PROTACs, where in one synthetic step, the POI binder, E3 binder, linker type and length can be explored.

Using the information generated by DNA-encoded chemistry screening, we were able to generate a small set of compounds with nM binding affinity. Attachment of a basic amine at the linker region converted these compounds from potent agonists into potent antagonists and further validated that we were targeting ERα directly.

Similar to bazedoxifene-based PROTACs, we also observed robust degradation with our novel ERα ligand with two peptidic ligands for VHL. We also demonstrated that this degradation was VHL-mediated by using a VHL ligand as a competitor and by also synthesizing the negative control PROTAC incorporating an inactive stereoisomer in the VHL-binding portion (see compound **18** *vs* **23**). Though the VHL amide and VHL phenoxy were nearly equivalent in their *in vitro* assay profiles, they behaved quite differently in PK studies, with markedly different AUC, CL_{obs}, and Vd_{ss}. We decided to progress a compound from each VHL variant (VHL

https://doi.org/10.1021/acs.jmedchem.1c00127
J. Med. Chem. 2021, 64, 5049−5066

amide and VHL-phenoxy) into the efficacy study and, aligned with the PK data, we observed, significant shrinkage in tumor volume with the phenoxy-linked PROTAC **21**.

For ERα, both monovalent (Fulvestrant and other second-generation SERDs) as well as PROTAC-based degraders seem to be viable approaches to ERα degradation. Both approaches have their advantages, wherein monovalent degraders are usually smaller and Lipinski rule compliant. However the rules of converting a target binding ligand into a monovalent degrader are not very well understood and the levels of degradation could vary widely. For PROTACs, their modular design allows for relatively simple construction, but the resulting molecules are usually large and need optimization of physiochemical properties. PROTACs may offer advantages of catalytic activity[46] and an acceptance of relatively weak POI binders.[42,47]

Overall, we have demonstrated that by utilizing our DECL platform, we were able to quickly identify very potent novel ERα binders that were efficiently incorporated into VHL-engaging PROTACs which demonstrated nanomolar ERα DC_{50} values with activity in ER-positive cells while demonstrating no effects in ER-negative cells. We also tested these compounds in normal immortalized breast cells and observed no off-target effects. The compounds also demonstrated suitable properties for *in vivo* applications and were efficacious in an ERα-dependent xenograft model. These compounds are valuable tools to further the development of novel ERα-based PROTAC-based therapeutics for patients with breast cancer.

EXPERIMENTAL SECTION

Construct Design and Cloning. The nucleotide sequences of the ligand-binding domains (LBD), containing amino acids 307−554, of ERα WT and the clinically relevant mutations D538G, S463P, and Y537S were synthesized with an N-terminal Avi-Tev-His tandem affinity tag and cloned into a pD454-SR *E. coli* expression vector by ATUM (Newark, CA, USA).

Protein Expression and Purification. Proteins were expressed in T7 Express cells for 12 h at 20 °C after induction with IPTG and then purified using standard Ni-NTA affinity chromatography followed by size exclusion chromatography.

Affinity-Mediated Selection of DNA-Encoded Chemical Libraries. Selections were performed as previously described.[48,49] Forty-four different DNA-encoded chemical libraries were combined and incubated with ERα WT, D538G, S463P, or Y537S. Separate incubations were set up with no target, ERα WT over a five-fold dilution series down from 7.7 μM to 24 nM, ERα WT at 7.7 μM with estradiol at 15 μM, and each of the D538G, S463P, and Y537S at 7.7 μM. After incubation, the mixtures were captured on His-Select IMAC matrix. After capture, the matrices were washed and then heat-eluted at 85 °C. The second round of selection was performed using the round-one eluate as an input and fresh proteins and estradiol repeating the conditions of the first round. The encoding DNA in the output of the second round of selection was amplified and then sequenced.

FP Binding Assay. Inhibition values for ERα compounds were determined using a fluorescent polarization (FP) assay. Compounds were pre-incubated with protein for 15 min, prior to the addition of the fluorescent ligand. The plates were further incubated at room temperature for 1 h and read on Spectramax Paradigm (λex 485 nm, λem 535 nm).

Cell Lines. Breast lines were obtained from the American Type Culture Collection: MCF7, MDA-MB231, T47D, ZR-75-1, and MCF10A and maintained in media specified by the ATCC.

Proliferation Assay. Cancer cells were seeded in hormone-deprived media and incubated for 72 h. In agonist mode, test compounds were added to the cells in a 10-point dose series in the same media. For antagonist mode, all wells (except the minimum signal control wells) were treated with 0.1 nM estradiol for 30 min followed by treatment with compounds. Plates were incubated a further 7 days at 37 °C, 5% CO_2, and then the cellular ATP content was measured using CellTiter-Glo 2.0 (Promega, Madison, WI) on a Tecan M1000 (Mannedorf, Switzerland). Once we began testing the PROTACs, the proliferation assay was run in complete media followed by compound treatment and a 7 day incubation period (results shown in Figure 3d).

Degradation Assay-ICW (Hormone-Deprived Media). MCF7 cells were seeded in hormone-deprived media and incubated for 72 h. Test compounds were added to the cells at 10-point dose series in hormone-deprived media. DMSO was dispensed into the maximum-signal control wells, and a compound control (**13**) was dispensed into the minimum-signal control wells to give a final concentration of 1 μM and were incubated a further 48 h. Cells were fixed with 4% formaldehyde, permeabilized with 0.1% Triton-X 100, and blocked with 3% fish gelatin. Primary antibodies (ERα and α-tubulin) were incubated overnight and secondary antibodies for 1 h before imaging on the Azure Biosystem Sapphire Biomolecular Imager (Dublin, CA).

Degradation Assay (Western Blotting). For western blots, 5×10^5 MCF7 cells in 2 mL of media per well were seeded into six-well plates 48 h before treatment. Cells were treated for the indicated times and doses, and western blot images were obtained through detection of rabbit anti-ERα (D6R2W, 1:1000, Cell Signaling Technologies, Danvers, MA) and mouse anti-β-actin (1:10000, Sigma) antibodies with goat anti-rabbit IRDye 800CW secondary antibody (1:10000, LI-COR) and donkey anti-mouse IRDye 680RD secondary antibody (1:10000, LI-COR) using an Azure Biosystems Sapphire Biomolecular Imager (Dublin, CA).

Gene Expression Analysis. MCF7 cells were seeded at 1.5×10^4 cells per well in 96-well plates in a volume of 90 μL complete media. Cell plates were incubated for 72 h. Test compounds were added in a 6-point dose series (10 μL). DMSO was dispensed into control wells, and Fulvestrant was dispensed as a reference (100 nM). All compounds were dosed for a final concentration of 0.5% DMSO (v/v). Cells with compound were further incubated for 24 h in humidified chambers at 37 °C, 5% CO_2. RNA was extracted, cDNA prepared, and qPCRs run using specific TaqMan probes (see Supplemental Methods). Data were analyzed using the QuantStudio Design & Analysis Software v1.4.3 using "Comparative C_T ($\Delta\Delta C_T$)" to analyze and export data to make dose−response curves in GraphPad Prism (San Diego, CA).[50]

ADME/PK. Determination of microsomal stability was performed at Pharmaron (Beijing, China). Test compounds (at 2 μM final concentration) were subjected to pooled human or male mouse liver microsomes, and % of compound remaining at 0, 15, 30, 45, and 60 min was measured and used to calculate an *in vitro* half-life (in minutes). PK studies were also performed at Pharmaron (Beijing, China) and were carried out according to the guidelines approved by the Institutional Animal Care and Use Committee (IACUC) of Pharmaron. Cassette iv (intravenous) PK was performed in male CD1 mice (3 mice per group) with up to five compounds each dosed at 0.3 mg/kg (dose volume of 2 mL/kg). The concentration of compounds was measured in plasma at nine timepoints (2, 5, 15, and 30 min and 1, 2, 4, 6, and 8 h post-dose), with 0.03 mL of blood collected via the dorsal metatarsal vein at each timepoint. Single dose sc (subcutaneous) PK was performed in male CD1 mice with each compound dosed at 10 mg/kg (dose volume of 10 mL/kg). The concentration of compounds was measured in plasma at nine timepoints (15 and 30 min and 1, 2, 4, 6, 8, 12, and 24 h post-dose), with 0.03 mL of blood collected via the dorsal metatarsal vein at each timepoint.

***In Vivo* Experiments.** All the procedures were performed according to the guidelines approved by the Institutional Animal Care and Use Committee (IACUC) of WuXi AppTec, Shanghai, China following the guidance of the Association for Assessment and Accreditation of Laboratory Animal Care (AAALAC). Each mouse was inoculated subcutaneously at the right flank with exponentially growing MCF-7 tumor cells (10×10^6) in 0.2 mL of PBS mixed with

https://doi.org/10.1021/acs.jmedchem.1c00127
J. Med. Chem. 2021, 64, 5049−5066

Matrigel (50:50) for tumor development. 17β-Estradiol (0.18 mg) pellets (Innovative Research of America) were implanted 2 days before cell inoculation. Sixty-four animals were randomized when the average tumor volume reached 165 mm^3 for the efficacy study. Each group consisted of eight randomly assigned tumor-bearing mice. Mice were dosed with vehicle, **18**, **21**, or Fulvestrant until the vehicle volume reached 2000 mm^3 as per IACUC guidelines. Tumor size was measured two times a week in two dimensions using a caliper, and the tumor volume (V) was expressed in mm^3 using the formula: $V = 0.5a \times b^2$, where a and b were the long and short diameters of the tumor, respectively. The mice were weighed every time prior to dosing. Tumor growth inhibition was calculated using the formula TGI (%) = (Vc − Vt)/(Vc −Vo) × 100, where Vc and Vt are the median of control and treated groups at the end of the study, respectively, and Vo at the start. Tumors were collected at the end of the study for PD analysis.

Synthetic Methods. All solvents and chemicals were used as purchased without further purification. All the reported yields are isolated yields. ^{1}H NMR spectra were recorded on a Bruker Advance spectrometer at 400 MHz for ^{1}H NMR. The chemical shift is expressed in ppm relative to tetramethylsilane (TMS) as an internal standard, and $CDCl_3$, DMSO-d_6, and CD_3OD were used as solvents. Multiplicity of peaks is expressed as s (singlet), d (doublet), t (triplet), q (quartet), dd (doublet of doublets), td (triplet of doublets), qd (quartet of doublets), dt (doublet of triplets), and m (multiplet). Compound identity and purity was assessed by LCMS using a Thermo UltiMate 3000 instrument, Phenomenex XB-C18 2.6 μM 2.1 × 30 mm column, mobile phase A: 99.9 acetonitrile/0.1 formic acid; mobile phase B: 99.9 water/0.1 formic acid. Elution was accomplished via a 7.0 min gradient beginning at 90:10 A/B and ending with 100% B with compounds identified by UV, λ = 254 nM, and ESI positive ion mass spectrometry. High-resolution mass spectrometry was acquired on an Agilent 6500 Q-TOF. All purities were >95%, unless specified (see supplemental for tabulation). NMR and MS data are consistent with in silico predicted values. See Supporting Information for LC-MS traces (**1**−**23**) and ^{1}H and ^{13}C NMR spectra for **18** and **21**.

2-Chloro-3-(((1-cyclopentyl-2,2,2-trifluoroethyl)(methyl)-amino)methyl)phenol (1). To a solution of 1-cyclopentyl-2,2,2-trifluoroethan-1-amine hydrochloride (406 mg, 2 mmol) and 2-chloro-3-hydroxybenzaldehyde (312 mg, 2 mmol) in MeOH (15 mL) was added AcOH (3 drops) and $NaBH_3CN$ (126 mg, 2 mmol). The reaction mixture was stirred at room temperature overnight, and then formaldehyde (2 mL, dissolved in water) was added to the solution, and the reaction mixture was stirred for an additional 2 h. The solvent was removed under reduced pressure to afford the residue, which was purified by prep-HPLC to obtain the title compound (164 mg, 25%) as a white solid. MS: (ESI) $[M + H]^+$ 322.24; ^{1}H NMR (400 MHz, DMSO-d_6) δ 7.12 (t, J = 7.6 Hz, 1H), 6.89 (t, J = 8.8 Hz, 2H), 3.89 (s, 2H), 3.33−3.10 (m, 1H), 2.29 (s, 3H), 2.23−2.17 (m, 1H), 1.86−1.24 (m, 8H).

2-Chloro-3-((((1-(2-fluorophenyl)cyclopentyl)methyl)-(methyl)amino)methyl)phenol (2). To a solution of (1-(2-fluorophenyl)cyclopentyl)methanamine (386 mg, 2 mmol) and 2-chloro-3-hydroxybenzaldehyde (312 mg, 2 mmol) in MeOH (15 mL) was added AcOH (3 drops) followed by $NaBH_3CN$ (126 mg, 2 mmol). The mixture was stirred at room temperature overnight, and then formaldehyde (2 mL, dissolved in water) was added to the solution, and the reaction mixture was stirred for an additional 2 h. The solvent was removed under reduced pressure to obtain a residue, which was purified by prep-HPLC to obtain the title compound (329 mg, 47%) as a white solid. MS: (ESI) $[M + H]^+$ 348.34; ^{1}H NMR (400 MHz, DMSO-d_6) δ 7.46−7.36 (m, 2H), 7.23−7.17 (m, 3H), 7.09 (d, J = 7.6 Hz, 1H), 7.01 (d, J = 7.2 Hz, 1H), 4.30 (d, J = 44.1 Hz, 2H), 3.54 (d, J = 22.8 Hz, 2H), 2.49 (s, 3H), 2.01−1.91 (m, 4H), 1.57−1.34 (m, 4H).

2-Chloro-3-((((1-(2-fluorophenyl)cyclopentyl)methyl)-(phenyl)amino)methyl)phenol (3). A solution of 1-(2-fluorophenyl)cyclopentane-1-carbaldehyde (200 mg, 1 mmol), aniline (93 mg, 1 mmol), $NaBH_3CN$ (126 mg, 2 mmol), and acetic acid (120 mg, 2 mmol) in methanol (5 mL) was stirred at room temperature overnight. The reaction mixture was concentrated under vacuum, and the residue was purified by column chromatography (20% EtOAc in petroleum ether with 1% TEA) to obtain N-((1-(2-fluorophenyl)-cyclopentyl)methyl)aniline (210 mg, 80%) as a colorless oil. MS: (ESI) $[M + H]^+$ 270.

A solution of N-((1-(2-fluorophenyl)cyclopentyl)methyl)aniline (210 mg, 0.8 mmol), 2-chloro-3-hydroxybenzaldehyde (125 mg, 0.8 mmol), $NaBH_3CN$ (100 mg, 1.6 mmol), and acetic acid (100 mg, 1.6 mmol) in methanol (5 mL) was stirred at room temperature overnight. The reaction mixture was concentrated under vacuum and the crude product was purified by prep-HPLC to obtain the title compound (30 mg, 9%) as a white solid. HPLC purity, 94.7%. MS: (ESI) $[M + H]^+$ 410.33; ^{1}H NMR (400 MHz, CD_3OD) δ 7.30−7.08 (m, 2H), 7.01 (ddd, J = 12.3, 6.7, 2.0 Hz, 4H), 6.87 (t, J = 7.9 Hz, 1H), 6.73 (dd, J = 8.0, 1.3 Hz, 1H), 6.60−6.49 (m, 3H), 6.42−6.34 (m, 1H), 4.19 (s, 2H), 3.74 (s, 2H), 2.25−2.12 (m, 2H), 2.08−1.96 (m, 2H), 1.93−1.79 (m, 2H), 1.77−1.63 (m, 2H).

2-Chloro-3-((((1-(2-fluorophenyl)cyclopentyl)methyl)(2-(piperidin-1-yl)ethyl)amino)methyl)phenol (4). To a solution of (1-(2-fluorophenyl)cyclopentyl)methanamine (300 mg, 1.55 mmol), 1-(2-chloroethyl)piperidine (228 mg,1.55 mmol) in acetonitrile (10 mL) was added potassium carbonate (212 mg,1.55 mmol). Then, the mixture was stirred at 80 °C for 2 h. The solution was concentrated under vacuum, and the residue was purified by silica gel column chromatography (5% MeOH in CH_2Cl_2) to obtain N-((1-(2-fluorophenyl)cyclopentyl)methyl)-2-(piperidin-1-yl)ethan-1-amine (400 mg, 85%) as a white solid. MS: (ESI) $[M + H]^+$ 305.

To a solution of N-((1-(2-fluorophenyl)cyclopentyl)methyl)-2-(piperidin-1-yl)ethan-1-amine (400 mg,1.31 mmol), 2-chloro-3-hydroxybenzaldehyde (204 mg,1.31 mmol) in MeOH (10 mL) was added acetic acid (1 mL). The mixture was stirred at room temperature for 5 h, and then $NaBH_3CN$ (83 mg, 1.31 mmol) was added. After stirring overnight, the reaction mixture was concentrated under vacuum, and the residue was purified by prep-HPLC to obtain the title compound (30 mg, 5%) as a white solid. MS: (ESI) $[M + H]^+$ 445.33; ^{1}H NMR (400 MHz, CD_3OD) δ = 7.40 (s, 1H), 7.27 (m, 1H), 7.07(m, 3H), 6.86 (m, 2H), 3.63 (s, 2H), 2.85(m, 8H), 2.52 (m, 1H), 2.01 (s, 2H), 1.87 (m, 2H), 1.45−1.57 (m, 9H)).

2-Chloro-3-((((1-(2-fluorophenyl)cyclopentyl)methyl)(3-(piperidin-1-yl)propyl)amino)methyl)phenol (5). To a solution of (1-(2-fluorophenyl)cyclopentyl)methanamine (300 mg, 1.55 mmol), 1-(3-chloropropyl)piperidine (250 mg, 1.55 mmol) in CH_3CN (10 mL) was added K_2CO_3 (212 mg, 1.55 mmol). The mixture was stirred at 80 °C for 2 h and then concentrated under vacuum. The residue was purified by column chromatography (5% MeOH in CH_2Cl_2) to obtain N-((1-(2-fluorophenyl)cyclopentyl)methyl)-3-(piperidin-1-yl)propan-1-amine (400 mg, 81%) as a white solid. MS: (ESI) $[M + H]^+$ 319.

To a solution of N-((1-(2-fluorophenyl)cyclopentyl)methyl)-3-(piperidin-1-yl)propan-1-amine (400 mg, 1.25 mmol), 2-chloro-3-hydroxybenzaldehyde (295 mg,1.25 mmol) in methanol (10 mL) was added AcOH (1 mL). The mixture was stirred at 25 °C for 5 h, and then $NaBH_3CN$ (79 mg, 1.25 mmol) was added to the solution. The solution was concentrated under vacuum and the residue was purified by prep-HPLC to obtain the title compound (30 mg, 5%) as a white solid. MS: (ESI) $[M + H]^+$ 459.24; ^{1}H NMR (400 MHz, CD_3OD) δ = 10.07 (s, 1H), 7.29 (m, 2H), 7.06 (m, 3H), 76.89(d, 1H), 6.82 (d, 1H), 3.40 (s, 2H), 3.22(d, 2H), 2.68 (m, 4H), 2.58 (s, 2H), 2.07 (m, 2H), 1.95 (s, 2H)), 1.71 (m, 6H), 1.32−1.50 (m, 6H).

2-Chloro-3-((((1-(2-fluorophenyl)cyclopentyl)methyl)(2-(2-(piperidin-1-yl)ethoxy)ethyl)amino)methyl)phenol (6). To a solution of 2-(2-(piperidin-1-yl)ethoxy)ethan-1-amine (172 mg, 1 mmol) and 1-(2-fluorophenyl)cyclopentane-1-carbaldehyde (192 mg, 1 mmol) in MeOH (20 mL) was added acetic acid (0.2 mL). The reaction mixture was stirred for 3 h, and then $NaBH_3CN$ (124 mg, 2 mmol) was added, and the reaction mixture was stirred overnight at room temperature. The reaction mixture was concentration under vacuum, and the crude product was purified by column chromatography (5% MeOH in CH_2Cl_2) to obtain N-((1-(2-fluorophenyl)-

https://doi.org/10.1021/acs.jmedchem.1c00127
J. Med. Chem. 2021, 64, 5049−5066

cyclopentyl)methyl)-2-(2-(piperidin-1-yl)ethoxy)ethan-1-amine (174 mg) as a yellow oil. MS: (ESI) $[M + H]^+$ 349.

To a solution of *N*-((1-(2-fluorophenyl)cyclopentyl)methyl)-2-(2-(piperidin-1-yl)ethoxy)ethan-1-amine (174 mg, 0.5 mmol) and 2-chloro-3-hydroxybenzaldehyde (78 mg, 0.5 mmol) in MeOH (20 mL) was added titanium(IV) isopropoxide (0.2 mL). The reaction mixture was stirred for 3 h, then $NaBH_3CN$ (92 mg, 1.5 mmol) was added, and the mixture was stirred overnight at room temperature. The reaction mixture was concentration under vacuum, and the crude product was purified by column chromatography (5% MeOH in CH_2Cl_2), and then by prep-HPLC to obtain the title compound (70 mg, 29%) as a white solid. MS: (ESI) $[M + H]^+$ 489.34; ^1H NMR (400 MHz, CD_3OD) δ 7.31 (td, J = 8.0, 1.7 Hz, 1H), 7.21 (ddd, J = 7.2, 4.9, 1.7 Hz, 1H), 7.10−6.96 (m, 3H), 6.92 (d, J = 6.2 Hz, 1H), 6.81 (dd, J = 8.0, 1.5 Hz, 1H), 3.59−3.53 (m, 4H), 3.48−3.34 (m, 4H), 3.23−3.19 (m, 2H), 3.14−2.87 (m, 2H), 2.85 (s, 2H), 2.41 (q, J = 6.4 Hz, 2H), 2.06 (d, J = 6.2 Hz, 2H), 1.95−1.67 (m, 7H), 1.62−1.42 (m, 5H).

2-Chloro-3-((((1-(2-fluorophenyl)cyclopentyl)methyl)(4-(2-(piperidin-1-yl)ethoxy)phenyl)amino)methyl)phenol (7). To a solution of 1-(2-fluorophenyl)cyclopentane-1-carboxylic acid (1 g, 5 mmol) in methanol (10 mL) was added $SOCl_2$ (1.2 g, 10 mmol) dropwise, and the solution was stirred overnight and then concentrated under vacuum. The residue was diluted with water (20 mL) and extracted with ethyl acetate (10 mL × 3). The combined organic layers were washed with $NaHCO_3$ (15 mL × 2) and brine (15 mL) and then dried over with anhydrous Na_2SO_4. After filtration, the solution was concentrated under vacuum to give methyl 1-(2-fluorophenyl)cyclopentane-1-carboxylate (1 g, crude) as a colorless oil, which was used directly in the next step. MS: (ESI) $[M + H]^+$ 223.

A solution of methyl 1-(2-fluorophenyl)cyclopentane-1-carboxylate (5 mmol) and $LiAlH_4$ (tetrahydrofuran solution, 2 M, 5 mL) in tetrahydrofuran (10 mL) was stirred for 2 h at room temperature. The reaction was quenched by $Na_2SO_4{\cdot}10H_2O$. After filtration, the filtrate was concentrated under vacuum, and the crude product was purified by column chromatography (1:15 methanol/dichloromethane) to obtain (1-(2-fluorophenyl)cyclopentyl)methanol (970 mg, 72%) as a colorless oil. MS: (ESI) $[M + H]^+$ 195.

A solution (1-(2-fluorophenyl)cyclopentyl)methanol (970 mg, 5 mmol), 2-iodoxybenzoic acid (1680 mg, 6 mmol), and DMSO (1 drop) in ethyl acetate (10 mL) was stirred at 80 °C overnight. The reaction mixture was filtered, and the filtrate was concentrated, diluted with water (20 mL), and extracted with ethyl acetate (10 mL × 3). The combined organic layers were washed with brine (15 mL × 3) and dried over with anhydrous Na_2SO_4. After filtration, the solution was concentrated under vacuum to obtain 1-(2-fluorophenyl)-cyclopentane-1-carbaldehyde (1 g, crude) as a colorless oil. MS: (ESI) $[M + H]^+$ 193.

A solution of 1-(2-fluorophenyl)cyclopentane-1-carbaldehyde (200 mg, 1 mmol), 4-(2-(piperidin-1-yl)ethoxy)aniline (220 mg, 1 mmol), $NaBH_3CN$ (126 mg, 2 mmol), and acetic acid (120 mg, 2 mmol) in methanol (5 mL) was stirred overnight at room temperature. The reaction mixture was concentrated under vacuum, and the crude product was purified by column chromatography (33% EtOAc in petroleum ether with 1% TEA) to obtain *N*-((1-(2-fluorophenyl)-cyclopentyl)methyl)-4-(2-(piperidin-1-yl)ethoxy)aniline (300 mg, 75%) as a colorless oil. MS: (ESI) $[M + H]^+$ 397.

A solution *N*-((1-(2-fluorophenyl)cyclopentyl)methyl)-4-(2-(piperidin-1-yl)ethoxy)aniline (300 mg, 0.8 mmol), 2-chloro-3-hydroxybenzaldehyde (125 mg, 0.8 mmol), $NaBH_3CN$ (100 mg, 1.6 mmol), and acetic acid (100 mg, 1.6 mmol) in MeOH (5 mL) was stirred at room temperature overnight. The reaction mixture was concentrated under vacuum, and the crude product was purified by prep-HPLC to obtain the title compound (40 mg, 10%) as a white solid. HPLC purity, 94.9%. MS: (ESI) $[M + H]^+$ 537.47; ^1H NMR (400 MHz, CD_3OD) δ 7.26−7.16 (m, 2H), 7.04−6.94 (m, 2H), 6.90 (t, J = 7.9 Hz, 1H), 6.72 (dd, J = 26.9, 20.0 Hz, 5H), 6.49 (d, J = 7.5 Hz, 1H), 4.23 (d, J = 15.5 Hz, 4H), 3.77 (s, 2H), 3.59 (d, J = 12.1 Hz, 2H), 3.52−3.45 (m, 2H), 3.13−2.96 (m, 2H), 2.34−1.90 (m, 7H), 1.90−1.73 (m, 5H), 1.73−1.47 (m, 2H).

2-Chloro-3-((methyl((1-(2-(2-(piperidin-1-yl)ethoxy)-phenyl)cyclopentyl)methyl)amino)methyl)phenol (8). To a solution of (1-(2-methoxyphenyl)cyclopentyl)methanamine (800 mg, 3.9 mmol) and $NaHCO_3$ (982 mg, 11.7 mmol) in THF (10 mL) and water (10 mL) was added $(Boc)_2O$ (1.7 g, 7.8 mmol). The reaction mixture was stirred overnight at room temperature and then concentrated in vacuo. The residue was extracted with dichloromethane (10 mL × 2), and the combined organic layers were dried over Na_2SO_4, concentrated in vacuo, and purified by column chromatography to obtain *tert*-butyl ((1-(2-methoxyphenyl)-cyclopentyl)methyl)carbamate (925 mg, 78%) as an oil. MS: (ESI) $[M + Na]^+$ 328.1.

To a solution of *tert*-butyl ((1-(2-methoxyphenyl)cyclopentyl)-methyl)carbamate (200 mg, 0.67 mmol) in THF (10 mL) at 0 °C was added NaH (47 mg, 1.97 mmol). The mixture was stirred at 0 °C for 30 min, and then MeI (186 mg, 1.310 mmol) was added. The mixture was stirred at room temperature overnight and then quenched with ice water (20 mL) and extracted with ethyl acetate (15 mL × 3). The combined organic layers were dried over Na_2SO_4, filtered, and concentrated, and the residue was purified by column chromatography to obtain *tert*-butyl ((1-(2-methoxyphenyl)cyclopentyl)-methyl)(methyl)carbamate (175 mg, 84%) as an oil. MS: (ESI) $[M + Na]^+$ 342.1.

To a solution of *tert*-butyl ((1-(2-methoxyphenyl)cyclopentyl)-methyl)(methyl)carbamate (175 mg, 0.56 mmol) in dichloromethane (8 mL) was added BBr_3 (278 mg, 1.11 mmol) at 0 °C. Then, the mixture was stirred at room temperature for 3 h. The solution was quenched with 1:9 ice water/methanol (10 mL) and extracted with dichloromethane (15 mL × 3). The combined organic layers were dried over Na_2SO_4, filtered, and concentrated, and the residue was purified by column chromatography to obtain 2-(1-((methylamino)-methyl)cyclopentyl)phenol (52 mg, 46%) as an oil. MS: (ESI) $[M + H]^+$ 206.1.

To a solution of 2-(1-((methylamino)methyl)cyclopentyl)phenol (52 mg, 0.253 mmol) and $NaHCO_3$ (64 mg, 0.759 mmol) in THF (5 mL) and water (5 mL) was added $(Boc)_2O$ (110 mg, 0.506 mmol). The reaction mixture was stirred overnight at room temperature and concentrated in vacuo, and the residue was acidified by 1 N HCl to pH = 3. The solution was extracted with ethyl acetate (10 mL × 2), and the combined organic layers were dried over Na_2SO_4, filtered, concentrated in vacuo, and purified by column chromatography to obtain *tert*-butyl ((1-(2-hydroxyphenyl)cyclopentyl)methyl)(methyl)-carbamate (50 mg, 77%) as an oil. MS: (ESI) $[M + Na]^+$ 328.1.

To a solution of *tert*-butyl ((1-(2-hydroxyphenyl)cyclopentyl)-methyl)(methyl)carbamate (47 mg, 0.154 mmol) and K_2CO_3 (64 mg, 0.462 mmol) in acetonitrile (5 mL) was added 1-(2-chloroethyl)-piperidine (34 mg, 0.231 mmol). The mixture was heated to 80 °C for 5 h and concentrated in vacuo, and the residue was purified by column chromatography to obtain *tert*-butyl methyl((1-(2-(2-(piperidin-1-yl)ethoxy)phenyl)cyclopentyl)methyl)carbamate (50 mg, 77%) as an oil. MS: (ESI) $[M + H]^+$ 417.3.

A solution of *tert*-butyl methyl((1-(2-(2-(piperidin-1-yl)ethoxy)-phenyl)cyclopentyl)methyl)carbamate (47 mg, 0.113 mmol) in HCl/dioxane (5 mL) was stirred at for 2 h at room temperature. The solution was concentrated in vacuo to obtain *N*-methyl-1-(1-(2-(2-(piperidin-1-yl)ethoxy)phenyl)cyclopentyl)methanamine (50 mg, crude) as an oil. LC-MS $(M + H)^+$ = 317.2.

A solution of *N*-methyl-1-(1-(2-(2-(piperidin-1-yl)ethoxy)phenyl)-cyclopentyl)methanamine (47 mg, 0.149 mmol) and 2-chloro-3-hydroxybenzaldehyde (35 mg, 0.224 mmol) in $Ti(OPr)_4$ (2 mL) was stirred for 4 h at room temperature. $NaBH_3CN$ (28 mg, 0.447 mmol) was added, and after stirring overnight at room temperature, the reaction was quenched with methanol (20 mL) and water (1 mL). The solid was removed by filtration, and the solution was concentrated in vacuo. The residue was purified by prep-HPLC to obtain the title compound (2.6 mg, 4%) as an off-white solid. MS: (ESI) $[M + H]^+$ 457.27; ^1H NMR (400 MHz, DMSO) δ 9.97 (s, 1H), 8.14 (s, 1H), 7.21−7.16 (m, 1H), 7.08−7.04 (m, 1H), 6.97 (d,

https://doi.org/10.1021/acs.jmedchem.1c00127
J. Med. Chem. 2021, 64, 5049−5066

1H), 6.88−6.76 (m, 3H), 4.19 (t, 2H), 3.38−3.32 (m, 4H), 3.18−3.13 (m, 2H), 2.89−2.80 (m, 3H), 2.75 (s, 2H), 2.12−2.08 (m, 2H), 1.79−1.68 (m, 9H), 1.51−1.48 (m, 5H).

2-Chloro-3-((((1-(2-fluoro-4-(2-(piperidin-1-yl)ethoxy)-phenyl)cyclopentyl)methyl)(methyl)amino)methyl)phenol (9). A solution of 2-(2-fluoro-4-methoxyphenyl)acetonitrile (1650 mg, 10 mmol), 1,4-dibromobutane (3210 mg, 15 mmol), and NaH (360 mg, 15 mmol) in dried DMF (10 mL) was stirred at room temperature for 6 h. After the reaction was completed, water (20 mL) was added 0 °C. The solution was concentrated, water was added, and the solution was extracted with CH_2Cl_2 (30 mL × 3). The combined organic layers were dried over with anhydrous Na_2SO_4, filtrated, and concentrated under reduced pressure, and the residue was purified by column chromatography to obtain 1-(2-fluoro-4-methoxyphenyl)-cyclopentane-1-carbonitrile (768 mg, 35%) as a white solid. MS: (ESI) $[M + H]^+$ 220.1.

A solution of 1-(2-fluoro-4-methoxyphenyl)cyclopentane-1-carbonitrile (760 mg, 3.47 mmol) and $LiAlH_4$ (132 mg, 3.47 mmol) in dried THF (10 mL) was stirred at 0 °C for 3 h. The reaction was completed by LC-MS, and $Na_2SO_4 \cdot 10\ H_2O$ (1117 mg, 3.47 mmol) was added to the solution at 0 °C. The solution was filtrated and concentrated to obtain (1-(2-fluoro-4-methoxyphenyl)cyclopentyl)methanamine (610 mg, 79%) as a white solid. MS: (ESI) $[M + H]^+$ 224.2.

To a solution of (1-(2-fluoro-4-methoxyphenyl)cyclopentyl)-methanamine (600 mg, 2.69 mmol) in dry CH_2Cl_2 (10 mL) at 0 °C was added BBr_3 (2 mL) dropwise, and then the mixture was stirred for 2 h until the product was detected by LC-MS. After the reaction was completed, water (10 mL) was added to the solution at 0 °C, and the solution extracted with CH_2Cl_2 (30 mL × 3), and the combined organic layer was dried over with anhydrous Na_2SO_4, filtrated, and then concentrated under vacuum to obtain 4-(1-(aminomethyl)cyclopentyl)-3-fluorophenol (368 mg, 65%) as a white oil. MS: (ESI) $[M + H]^+$ 210.1.

A solution of 4-(1-(aminomethyl)cyclopentyl)-3-fluorophenol (360 mg, 1.72 mmol), Boc_2O (376 mg, 1.72 mmol), $NaHCO_3$ (168 mg, 2 mmol) in THF (10 mL), and water (2 mL) was stirred at room temperature for 3 h. The solution was concentrated, diluted with water, and extracted with CH_2Cl_2 (20 mL × 3), and the combined organic layers were dried over with anhydrous Na_2SO_4, filtrated, and concentrated under vacuum, and the crude product was purified using column chromatography to obtain *tert*-butyl ((1-(2-fluoro-4-hydroxyphenyl)cyclopentyl)methyl)carbamate (185 mg, 35%) as a white solid. MS: (ESI) $[M + H\text{-}t\text{Bu}]^+$ 254.2.

A solution *tert*-butyl ((1-(2-fluoro-4-hydroxyphenyl)cyclopentyl)-methyl)carbamate (170 mg, 0.55 mmol), 1-(2-chloroethyl)piperidine (88 mg, 0.6 mmol), and Cs_2CO_3 (196 mg, 0.6 mmol) in DMF (10 mL) was stirred at 100 °C for 3 h. The reaction mixture was cooled, concentrated, diluted with water, and extracted with CH_2Cl_2 (20 mL × 3). The combined organic layers were dried over with anhydrous Na_2SO_4 and filtrated, and the residue was purified by column chromatography to obtain *tert*-butyl ((1-(2-fluoro-4-(2-(piperidin-1-yl)ethoxy)phenyl)cyclopentyl)methyl)carbamate (118 mg, 51%) as a white solid. MS: (ESI) $[M + H]^+$ 421.3.

A solution of *tert*-butyl ((1-(2-fluoro-4-(2-(piperidin-1-yl)ethoxy)-phenyl)cyclopentyl)methyl)carbamate (118 mg, 0.28 mmol) in 1,4-dioxane HCl (4 M, 5 mL) was stirred at room temperature. After 2 h, the solution was concentrated to obtain (1-(2-fluoro-4-(2-(piperidin-1-yl)ethoxy)phenyl)cyclopentyl)methanamine (85 mg, 95%) as a white solid. MS: (ESI) $[M + H]^+$ 321.2.

A solution of 2-chloro-3-hydroxybenzaldehyde (47 mg, 0.3 mmol), (1-(2-fluoro-4-(2-(piperidin-1-yl)ethoxy)phenyl)cyclopentyl)-methanamine (85 mg, 0.27 mmol) in AcOH (0.2 mL), and MeOH (10 mL) was stirred for 2 h at room temperature. Then, $NaBH_3CN$ (19 mg, 0.3 mmol) was added, and the reaction mixture was stirred overnight. Paraformaldehyde (12 mg, 0.4 mmol) was added, and the mixture was stirred for 2 h. Then, another aliquot of $NaBH_3CN$ (19 mg, 0.3 mmol) was added and stirring was continued at room temperature for 5 h. After the reaction was completed, the solution was concentrated diluted with water and extracted with CH_2Cl_2 (20 mL × 3). The combined organic layers were dried over with anhydrous Na_2SO_4, filtrated, and concentrated under vacuum, and the residue was purified by column chromatography followed by prep-HPLC to obtain the title compound (35 mg, 27%) as a white solid. MS: (ESI) $[M + H]^+$ 475.27; ^1H NMR (400 MHz, MeOD) δ 7.33−7.29 (m, 1H), 7.13−7.10 (m, 1H), 6.93−6.91 (m, 2H), 6.78−6.74 (m, 2H), 4.35 (s, 2H), 3.80 (s, 2.67H), 3.54−3.50 (m, 2.36H), 3.15 (s, 3H), 2.32 (s, 3H), 2.04−1.90 (m, 8H), 1.71−1.63 (m, 6H).

3-(((4-(2-Azidoethoxy)phenyl)((1-(2-fluorophenyl)-cyclopentyl)methyl)amino)methyl)-2-chlorophenol (Intermediate 7-Azide). To a solution of 2-(4-aminophenoxy)ethan-1-ol (306 mg, 2 mmol) and $(Boc)_2O$ (436 mg, 2 mmol) in THF (20 mL) was added K_2CO_3 (828 mg, 6 mmol). The reaction mixture was stirred overnight and then concentrated under vacuum. The residue was diluted with water (30 mL) and extracted with ethyl acetate (30 mL × 3). The combined organic layers were washed with brine (25 mL × 3) and then dried over with anhydrous Na_2SO_4. After filtration, the solution was concentration under vacuum, and the crude product was purified by column chromatography (5% MeOH in DCM) to obtain *tert*-butyl (4-(2-hydroxyethoxy)phenyl)carbamate (540 mg, crude) as a yellow oil. MS: (ESI) $[M + H]^+$ 254.

To a solution of *tert*-butyl (4-(2-hydroxyethoxy)phenyl)carbamate (540 mg, crude) in DCM (20 mL) was added MsCl (0.5 mL) and DIEA (1 mL). The reaction mixture was stirred for 1 h, and then the reaction mixture was washed with brine (25 mL × 3) and dried over with anhydrous Na_2SO_4. After filtration, the solution was concentration under vacuum to a obtain 2-(4-((*tert*-butoxycarbonyl)amino)-phenoxy)ethyl methanesulfonate (470 mg) as a yellow oil. MS: (ESI) $[M + H]^+$ 332.

To a solution of 2-(4-((*tert*-butoxycarbonyl)amino)phenoxy)ethyl methanesulfonate (470 mg, crude) in DMF (10 mL) was added NaN_3 (650 mg, 10 mmol). The reaction mixture was stirred at 60 °C overnight. The reaction mixture was diluted with water (50 mL) and extracted with ethyl acetate (30 mL × 3). The combined organic layer was washed with brine (30 mL × 3) and then dried over with anhydrous Na_2SO_4. After filtration, the solution was concentration under vacuum to give a crude *tert*-butyl (4-(2-azidoethoxy)phenyl)-carbamate (530 mg, crude) as a yellow oil. MS: (ESI) $[M + H]^+$ 279.

To a solution of *tert*-butyl (4-(2-azidoethoxy)phenyl)carbamate (200 mg, crude) in DMF (10 mL) was added TFA (1 mL). The reaction mixture was stirred at room temperature for 2 h and then concentrated under vacuum to obtain crude 4-(2-azidoethoxy)aniline (350 mg, crude) as a yellow oil. MS: (ESI) $[M + H]^+$ 179.

To a solution of 4-(2-azidoethoxy)aniline (300 mg, crude) and 1-(2-fluorophenyl)cyclopentane-1-carbaldehyde (192 mg, 1 mmol) in MeOH (20 mL) was added acetic acid (0.2 mL). The reaction mixture was stirred at room temperature for 3 h. Then, $NaBH_3CN$ (124 mg, 2 mmol) was added and the reaction mixture was stirred overnight. The reaction mixture was concentration under vacuum, and the crude product was purified by column chromatography (5% MeOH in DCM) to obtain 4-(2-azidoethoxy)-*N*-((1-(2-fluorophenyl)cyclopentyl)methyl)aniline (390 mg) as a yellow oil. MS: (ESI) $[M + H]^+$ 355.

To a solution of 4-(2-azidoethoxy)-*N*-((1-(2-fluorophenyl)-cyclopentyl)methyl)aniline (350 mg, crude) and 1-(2-fluorophenyl)-cyclopentane-1-carbaldehyde (78 mg, 0.5 mmol) in MeOH (20 mL) was added AcOH (0.2 mL), and the reaction mixture was stirred overnight. Then, $NaBH_3CN$ (124 mg, 2 mmol) was added, and the reaction mixture was stirred overnight at room temperature. The reaction mixture was concentrated and then purified by prep-HPLC to obtain the title intermediate (110 mg) as a colorless oil. MS: (ESI) $[M + H]^+$ 489. ^1H NMR (400 MHz, CD_3OD) δ 7.30−7.16 (m, 2H), 7.04−6.97 (m, 2H), 6.90 (t, J = 7.9 Hz, 1H), 6.73 (dd, J = 8.0, 1.2 Hz, 1H), 6.70−6.64 (m, 2H), 6.54 (d, J = 9.2 Hz, 2H), 6.47 (d, J = 7.6 Hz, 1H), 4.15 (s, 2H), 4.05−4.00 (m, 2H), 3.69 (s, 2H), 3.52−3.48 (m, 2H), 2.23−2.13 (m, 2H), 2.05−1.95 (m, 2H), 1.88−1.76 (m, 2H), 1.75−1.63 (m, 2H).

General Procedure for Huisgen 1,3-Diploar Cycloaddition. Equal volumes of 200 mM THPTA aqueous solution and 100 mM $CuSO_4 \cdot 5H_2O$ aqueous solution were combined, vortexed and let stand for 5 min. Separately, 1 mL of azide solution (25 mM in

https://doi.org/10.1021/acs.jmedchem.1c00127
J. Med. Chem. 2021, 64, 5049−5066

DMSO) and 1 mL of alkyne solution (25 mM) were added to a reaction vial, vortexed, and then 75 μL of the premixed THPTA/$CuSO_4 \cdot 5H_2O$ solution was added, followed by 225 μL of sodium ascorbate solution (100 mM in water). The reaction mixture was vortexed and then the reaction was monitored by LCMS. If necessary the reaction was heated to 50 °C overnight. After reaction completion, the cooled reaction mixture was loaded directly and purified by a mass triggered Waters LCMS reversed phase purification system using water/acetonitrile/0.1% formic acid as an eluent. The fractions were dried by lyophilization to afford the title compound as a solid.

2-(2,6-Dioxopiperidin-3-yl)-4-(2-((1-(2-(4-((5-hydroxy-2-(4-hydroxyphenyl)-3-methyl-1H-indol-1-yl)methyl)phenoxy)ethyl)-1H-1,2,3-triazol-4-yl)methoxy)ethoxy)isoindoline-1,3-dione (**10**). Following General Procedure using 1-(4-(2-azidoethoxy)benzyl)-2-(4-hydroxyphenyl)-3-methyl-1*H*-indol-5-ol (10.4 mg, 0.025 mmol) and 2-(2,6-dioxopiperidin-3-yl)-4-(2-(prop-2-yn-1-yloxy)ethoxy)-isoindoline-1,3-dione (8.9 mg, 0.025 mmol) to obtain the title compound (14.5 mg, 75% yield). MS: (ESI) $[M + H]^+$ 771.42.

(2S,4R)-4-Hydroxy-1-((S)-2-(2-((1-(2-(4-((5-hydroxy-2-(4-hydroxyphenyl)-3-methyl-1H-indol-1-yl)methyl)phenoxy)ethyl)-1H-1,2,3-triazol-4-yl)methoxy)acetamido)-3,3-dimethylbutanoyl)-N-((S)-1-(4-(4-methylthiazol-5-yl)phenyl)ethyl)pyrrolidine-2-carboxamide (**11**). Following General Procedure using 1-(4-(2-azidoethoxy)-benzyl)-2-(4-hydroxyphenyl)-3-methyl-1*H*-indol-5-ol (10.4 mg, 0.025 mmol) and (2*S*,4*R*)-1-((*S*)-2-(1-fluorocyclopropane-1-carboxamido)-3,3-dimethylbutanoyl)- 4-hydroxy-*N*-(4-(4-methylthiazol-5-yl)-2-(2-(prop-2-yn-1-yloxy)ethoxy)benzyl)pyrrolidine-2-carboxamide (13.5 mg, 0.025 mmol) to obtain the title compound (21.2 mg, 89% yield). MS: (ESI) $[M + H]^+$ 955.43.

(2S,4R)-4-Hydroxy-1-((S)-2-(2-(2-((1-(2-(4-((5-hydroxy-2-(4-hydroxyphenyl)-3-methyl-1H-indol-1-yl)methyl)phenoxy)ethyl)-1H-1,2,3-triazol-4-yl)methoxy)ethoxy)acetamido)-3,3-dimethylbutanoyl)-N-((S)-1-(4-(4-methylthiazol-5-yl)phenyl)ethyl)pyrrolidine-2-carboxamide (**12**). Following General Procedure using 1-(4-(2-azidoethoxy)benzyl)-2-(4-hydroxyphenyl)-3-methyl-1*H*-indol-5-ol solution (10.4 mg, 0.025 mmol) and (2*S*,4*R*)-1-((*S*)-3,3-dimethyl-2-(2-(2-(prop-2-yn-1-yloxy)ethoxy)acetamido)butanoyl)-4-hydroxy-*N*-((*S*)-1-(4-(4-methylthiazol-5-yl)phenyl)ethyl)pyrrolidine-2-carboxamide solution (14.6 mg, 0.025 mmol) to afford the title compound (22.2 mg, 89% yield). MS: (ESI) $[M + H]^+$ 999.38.

(2S,4R)-1-((S)-12-(tert-Butyl)-1-(1-(2-(4-((5-hydroxy-2-(4-hydroxyphenyl)-3-methyl-1H-indol-1-yl)methyl)phenoxy)ethyl)-1H-1,2,3-triazol-4-yl)-10-oxo-2,5,8-trioxa-11-azatridecan-13-oyl)-4-hydroxy-N-((S)-1-(4-(4-methylthiazol-5-yl)phenyl)ethyl)pyrrolidine-2-carboxamide (**13**). Following General Procedure using 1-(4-(2-azidoethoxy)benzyl)-2-(4-hydroxyphenyl)-3-methyl-1*H*-indol-5-ol (10.4 mg, 0.025 mmol) and (2*S*,4*R*)-1-((*S*)-2-(*tert*-butyl)-4-oxo-6,9,12-trioxa-3-azapentadec-14-ynoyl)-4-hydroxy-*N*-((*S*)-1-(4-(4-methylthiazol-5-yl)phenyl)ethyl)pyrrolidine-2-carboxamide (15.7 mg, 0.025 mmol) to afford the title compound (22.3 mg, 86%). MS: (ESI) $[M + H]^+$ 1043.43.

(2S,4R)-1-((S)-2-(1-Fluorocyclopropane-1-carboxamido)-3,3-dimethylbutanoyl)-4-hydroxy-N-(2-(2-((1-(2-(4-((5-hydroxy-2-(4-hydroxyphenyl)-3-methyl-1H-indol-1-yl)methyl)phenoxy)ethyl)-1H-1,2,3-triazol-4-yl)methoxy)ethoxy)-4-(4-methylthiazol-5-yl)benzyl)-pyrrolidine-2-carboxamide (**14**). Following General Procedure using 1-(4-(2-azidoethoxy)benzyl)-2-(4-hydroxyphenyl)-3-methyl-1*H*-indol-5-ol and (2*S*,4*R*)-1-((*S*)-2-(1-fluorocyclopropane-1-carboxamido)-3,3-dimethylbutanoyl)-4-hydroxy-*N*-(4-(4-methylthiazol-5-yl)-2-(2-(prop-2-yn-1-yloxy)ethoxy)benzyl)pyrrolidine-2-carboxamide to obtain the title compound (55 mg, 71%). MS: (ESI) $[M + H]^+$ 1029.26.

(S)-N-((S)-1-Cyclohexyl-2-((S)-2-(4-(3-(2-((1-(2-(4-((5-hydroxy-2-(4-hydroxyphenyl)-3-methyl-1H-indol-1-yl)methyl)phenoxy)ethyl)-1H-1,2,3-triazol-4-yl)methoxy)ethoxy)benzoyl)thiazol-2-yl)-pyrrolidin-1-yl)-2-oxoethyl)-2-(methylamino)propanamide (**15**). Following General Procedure using 1-(4-(2-azidoethoxy)benzyl)-2-(4-hydroxyphenyl)-3-methyl-1*H*-indol-5-ol and (*S*)-*N*-((*S*)-1-cyclohexyl-2-oxo-2-((*S*)-2-(4-(3-(2-(prop-2-yn-1-yloxy)ethoxy)benzoyl)-thiazol-2-yl)pyrrolidin-1-yl)ethyl)-2-(methylamino)propanamide to obtain the title compound as the formic salt. MS: (ESI) $[M + H]^+$ 995.47.

(S)-N-((S)-2-((S)-2-(4-(4-Fluorobenzoyl)thiazol-2-yl)pyrrolidin-1-yl)-1-(1-(2-(2-((1-(2-(4-((5-hydroxy-2-(4-hydroxyphenyl)-3-methyl-1H-indol-1-yl)methyl)phenoxy)ethyl)-1H-1,2,3-triazol-4-yl)-methoxy)ethoxy)acetyl)piperidin-4-yl)-2-oxoethyl)-2-(methylamino)propanamide (**16**). To a solution of 1-(4-(2-azidoethoxy)benzyl)-2-(4-hydroxyphenyl)-3-methyl-1*H*-indol-5-ol (22 mg, 0.053 mmol) and (*S*)-*N*-((*S*)-2-((S)-2-(4-(4-fluorobenzoyl)-thiazol-2-yl)pyrrolidin-1-yl)-2-oxo-1-(1-(2-(2-(prop-2-yn-1-yloxy)-ethoxy)acetyl)piperidin-4-yl)ethyl)-2-(methylamino)propanamide (21 mg, 0.033 mmol) in DMSO (2 mL) was added 0.08 mL of premixed aqueous solution of $CuSO_4 \cdot 5H_2O$ (100 mM, 0.04 mL) and THPTA (200 mM, 0.04 mL), and the mixture was stirred at room temperature for 2 min followed by the addition of sodium ascorbate (100 mM, 0.225 mL). The combined mixture was then shaken at 50 °C for 12 h. The cooled reaction mixture was loaded directly onto the Waters LCMS reversed phase purification system using water/acetonitrile/0.1% FA as an eluent. The fractions were dried by lyophilization to afford the title compound as the formate salt (14.7 mg, 42% yield). MS: (ESI) $[M + H]^+$ 1056.37.

(2S,4R)-1-((S)-2-(2-((1-(2-(4-((2-Chloro-3-hydroxybenzyl)((1-(2-fluorophenyl)cyclopentyl)methyl)amino)phenoxy)ethyl)-1H-1,2,3-triazol-4-yl)methoxy)acetamido)-3,3-dimethylbutanoyl)-4-hydroxy-N-((S)-1-(4-(4-methylthiazol-5-yl)phenyl)ethyl)pyrrolidine-2-carboxamide (**17**). Following General Procedure using 3-(((4-(2-azidoethoxy)phenyl)((1-(2-fluorophenyl)cyclopentyl)methyl)-amino)methyl)-2-chlorophenol (12.4 mg, 0.025 mmol) and (2*S*,4*R*)-1-((*S*)-3,3-dimethyl-2-(2-(prop-2-yn-1-yloxy)acetamido)butanoyl)-4-hydroxy-*N*-((*S*)-1-(4-(4-methylthiazol-5-yl)phenyl)ethyl)pyrrolidine-2-carboxamide (13.5 mg, 0.025 mmol) to afford the title compound as the formic acid salt (9.6 mg, 35% yield). MS: (ESI) $[M + H]^+$ 1035.35.

(2S,4R)-1-((S)-2-(2-(2-((1-(2-(4-((2-Chloro-3-hydroxybenzyl)((1-(2-fluorophenyl)cyclopentyl)methyl)amino)phenoxy)ethyl)-1H-1,2,3-triazol-4-yl)methoxy)ethoxy)acetamido)-3,3-dimethylbutanoyl)-4-hydroxy-N-((S)-1-(4-(4-methylthiazol-5-yl)phenyl)ethyl)-pyrrolidine-2-carboxamide (**18**). To a solution of 3-(((4-(2-azidoethoxy)phenyl)((1-(2-fluorophenyl)cyclopentyl)methyl)-amino)methyl)-2-chlorophenol(372 mg, 0.75 mmol) and (2*S*,4*R*)-1-((*S*)-3,3-dimethyl-2-(2-(2-(prop-2-yn-1-yloxy)ethoxy)acetamido)-butanoyl)-4-hydroxy-*N*-((*S*)-1-(4-(4-methylthiazol-5-yl)phenyl)-ethyl)pyrrolidine-2-carboxamide (422 mg, 0.723 mmol) in DMSO (15 mL) was added 0.8 mL of premixed aqueous solution of $CuSO_4$ (100 mM, 0.4 mL) and THPTA (200 mM, 0.4 mL), and the mixture was stirred at room temperature for 2 min followed by the addition of sodium ascorbate (100 mM, 2.25 mL). The combined mixture was then stirred at 25 °C for 12 h. The mixture was diluted with water (30 mL) and extracted with EtOAc (30 mL × 2), and the organic phase was washed with brine (20 mL), dried over anhydrous Na_2SO_4, concentrated to an oil, and purified over silica gel column chromatography eluted with DCM/MeOH (gradient) to obtain the title compound as a white solid (777 mg, 96% yield). MS: (ESI) $[M + H]^+$ 1079.37; HRMS (ES^+) for $C_{57}H_{68}ClFN_8O_8S$ $(M + H)^+$: calcd 1079.4632; found 1079.4646; ^1H NMR (400 MHz, DMSO-d_6) δ ppm 0.92 (s, 9H), 1.35 (d, J = 7.03 Hz, 3H), 1.57 (br s, 2H), 1.65−1.81 (m, 3H), 1.84−1.96 (m, 2H), 1.97−2.10(m, 3H), 2.45 (s, 3H), 3.55−3.68 (m, 8H), 3.95 (s, 2H), 4.05 (s, 2H), 4.17−4.31 (m, 3H), 4.45 (t, J = 8.28 Hz, 1H), 4.52−4.62 (m, 3H), 4.66 (br t, J = 4.89 Hz, 2H), 4.90 (br t, J = 7.15 Hz, 1H), 5.13 (d, J = 3.51 Hz, 1H), 6.30 (d, J = 7.53 Hz, 1H), 6.42−6.51 (m, 2H), 6.60−6.65 (m, 2H), 6.75 (d, J = 7.28 Hz, 1H), 6.90 (t, J = 7.78 Hz, 1H), 7.03−7.12 (m, 2H), 7.18−7.29 (m, 2H), 7.33−7.46 (m, 5H), 8.12−8.17 (m, 1H), 8.44 (d, J = 7.53 Hz, 1H), 8.98 (s, 1 H), 10.03 (s, 1H).

(2S,4R)-1-((S)-12-(tert-Butyl)-1-(1-(2-(4-((2-chloro-3-hydroxybenzyl)((1-(2-fluorophenyl)cyclopentyl)methyl)amino)-phenoxy)ethyl)-1H-1,2,3-triazol-4-yl)-10-oxo-2,5,8-trioxa-11-aza-tridecan-13-oyl)-4-hydroxy-N-((S)-1-(4-(4-methylthiazol-5-yl)-phenyl)ethyl)pyrrolidine-2-carboxamide (**19**). Following General Procedure using 3-(((4-(2-azidoethoxy)phenyl)((1-(2-fluorophenyl)-cyclopentyl)methyl)amino)methyl)-2-chlorophenol (12.4 mg, 0.025

https://doi.org/10.1021/acs.jmedchem.1c00127
J. Med. Chem. 2021, 64, 5049−5066

mmol) and (2S,4R)-1-((S)-2-(*tert*-butyl)-4-oxo-6,9,12-trioxa-3-azapentadec-14-ynoyl)-4-hydroxy-*N*-((S)-1-(4-(4-methylthiazol-5-yl)-phenyl)ethyl)pyrrolidine-2-carboxamide (15.7 mg, 0.025 mmol) to obtain the title compound as a formate salt (1.5 mg, 5%). MS: (ESI) $[M + H]^+$ 1123.25.

(2S,4R)-N-(2-(2-((1-(2-(4-((2-Chloro-3-hydroxybenzyl)((1-(2-fluorophenyl)cyclopentyl)methyl)amino)phenoxy)ethyl)-1H-1,2,3-triazol-4-yl)methoxy)ethoxy)-4-(4-methylthiazol-5-yl)benzyl)-1-((S)-2-(1-fluorocyclopropane-1-carboxamido)-3,3-dimethylbutanoyl)-4-hydroxypyrrolidine-2-carboxamide (**20**). Following General Procedure using 3-(((4-(2-azidoethoxy)phenyl)((1-(2-fluorophenyl)-cyclopentyl)methyl)amino)methyl)-2-chlorophenol (12.4 mg, 0.025 mmol) and (2S,4R)-1-((S)-2-(1-fluorocyclopropane-1-carboxamido)-3,3-dimethylbutanoyl)-4-hydroxy-*N*-(4-(4-methylthiazol-5-yl)-2-(2-(prop-2-yn-1-yloxy)ethoxy)benzyl)pyrrolidine-2-carboxamide (15.4 mg, 0.025 mmol) to obtain the title compound as the formic acid salt (9.4 mg, 29%). MS: (ESI) $[M + H]^+$ 1109.38.

(2S,4R)-N-(2-(2-(2-((1-(2-(4-((2-Chloro-3-hydroxybenzyl)((1-(2-fluorophenyl)cyclopentyl)methyl)amino)phenoxy)ethyl)-1H-1,2,3-triazol-4-yl)methoxy)ethoxy)ethoxy)-4-(4-methylthiazol-5-yl)-benzyl)-1-((S)-2-(1-fluorocyclopropane-1-carboxamido)-3,3-dimethylbutanoyl)-4-hydroxypyrrolidine-2-carboxamide (**21**). To a solution of 3-(((4-(2-azidoethoxy)phenyl)((1-(2-fluorophenyl)-cyclopentyl)methyl)amino)methyl)-2-chlorophenol (421 mg, 0.85 mmol) and (2S,4R)-1-((S)-2-(1-fluorocyclopropane-1-carboxamido)-3,3-dimethylbutanoyl)-4-hydroxy-*N*-(4-(4-methylthiazol-5-yl)-2-(2-(2-(prop-2-yn-1-yloxy)ethoxy)ethoxy)benzyl)pyrrolidine-2-carboxamide (519 mg, 0.788 mmol) in DMSO (15 mL) was added 0.8 mL of premixed aqueous solution of $CuSO_4$ (100 mM, 0.4 mL) and THPTA (200 mM, 0.4 mL), and the mixture was stirred at room temperature for 2 min followed by the addition of sodium ascorbate (100 mM, 2.25 mL). The combined mixture was then stirred at 25 °C for 12 h. The mixture was diluted with water (30 mL), extracted with EtOAc (30 mL x 2), the organic phase was washed with brine (20 mL), dried over anhydrous Na_2SO_4, concentrated to an oil, and purified over silica gel column chromatography eluted with DCM/MeOH (gradient) to obtain the title compound as a white solid (864 mg, 95%). MS: (ESI) $[M + H]^+$ 1153.41; HRMS (ES^+) for $C_{60}H_{71}ClF_2N_8O_9S$ $(M + H)^+$: calcd 1153.4800; found 1153.4794; ^1H NMR (400 MHz, DMSO-d_6) δ ppm 0.93 (s, 9H), 1.10−1.28 (m, 2H), 1.29−1.43 (m, 2H), 1.57 (m, 2H), 1.73 (m, 2H), 1.84−1.92 (m, 3H), 1.99−2.12 (m, 3H), 2.43 (s, 3H), 3.56−3.67 (m, 8H), 3.71−3.83 (m, 2H), 4.04 (s, 2H), 4.12−4.23 (m, 5H), 4.25−4.38 (m, 2H), 4.46−4.55 (m, 3H), 4.56−4.70 (m, 3H), 5.17 (d, J = 3.51 Hz, 1H), 6.30 (d, J = 7.53 Hz, 1H), 6.45 (m, J = 9.03 Hz, 2H), 6.61 (m, J = 9.03 Hz, 2H), 6.75 (d, J = 7.03 Hz, 1H), 6.89 (t, J = 7.41 Hz, 1H), 6.96 (d, J = 7.26 Hz, 1H), 7.01−7.11 (m, 3H), 7.18−7.32 (m, 3H), 7.41 (d, J = 8.03 Hz, 1H), 8.09 (s, 1H), 8.49 (t, J = 5.90 Hz, 1H), 8.97 (s, 1H), 10.03 (s, 1H).

(2S,4R)-N-(2-(2-(2-(2-((1-(2-(4-((2-Chloro-3-hydroxybenzyl)((1-(2-fluorophenyl)cyclopentyl)methyl)amino)phenoxy)ethyl)-1H-1,2,3-triazol-4-yl)methoxy)ethoxy)ethoxy)ethoxy)-4-(4-methylthiazol-5-yl)benzyl)-1-((S)-2-(1-fluorocyclopropane-1-carboxamido)-3,3-dimethylbutanoyl)-4-hydroxypyrrolidine-2-carboxamide (**22**). Following General Procedure using 3-(((4-(2-azidoethoxy)phenyl)((1-(2-fluorophenyl)cyclopentyl)methyl)amino)methyl)-2-chlorophenol (12.4 mg, 0.025 mmol) and (2S,4R)-1-((S)-2-(1-fluorocyclopropane-1-carboxamido)-3,3-dimethylbutanoyl)-4-hydroxy-*N*-(4-(4-methylthiazol-5-yl)-2-(2-(2-(2-(prop-2-yn-1-yloxy)ethoxy)ethoxy)ethoxy)-benzyl)pyrrolidine-2-carboxamide (17.6 mg, 0.025 mmol) to obtain the title compound as a formate salt (5.5 mg, 18% yield). MS: (ESI) $[M + H]^+$ 1197.38.

(2S,4S)-1-((S)-2-(2-(2-((1-(2-(4-((2-Chloro-3-hydroxybenzyl)((1-(2-fluorophenyl)cyclopentyl)methyl)amino)phenoxy)ethyl)-1H-1,2,3-triazol-4-yl)methoxy)ethoxy)acetamido)-3,3-dimethylbutanoyl)-4-hydroxy-N-((S)-1-(4-(4-methylthiazol-5-yl)phenyl)ethyl)pyrrolidine-2-carboxamide (**23**). Following General Procedure using 3-(((4-(2-azidoethoxy)phenyl)((1-(2-fluorophenyl)cyclopentyl)methyl)-amino)methyl)-2-chlorophenol and (2S,4S)-1-((S)-3,3-dimethyl-2-(2-(2-(prop-2-yn-1-yloxy)ethoxy)acetamido)butanoyl)-4-hydroxy-*N*-((S)-1-(4-(4-methylthiazol-5-yl)phenyl)ethyl)pyrrolidine-2-carboxamide to afford the title compound as the formic acid salt. MS: (ESI) $[M + H]^+$ 1079.40.

■ ASSOCIATED CONTENT

Supporting Information

The Supporting Information is available free of charge at https://pubs.acs.org/doi/10.1021/acs.jmedchem.1c00127.

Denaturing gel of proteins, LC-MS for compounds **1**−**23** (parent ion, retention time, purity, and chromatograms), ^1H and ^{13}C NMR spectra for compounds **18** and **21**, supplemental figures demonstrating purification of ERα proteins and degradation of ERα in ER+ breast cancer cells, and supplemental methods giving detailed protocols for protein production, biochemical and cellular assays, and DECL screening (PDF)

Molecular formula strings and biological data (CSV)

■ AUTHOR INFORMATION

Corresponding Authors

Jeremy S. Disch − *X-Chem Inc., Waltham, Massachusetts 02453, United States*; orcid.org/0000-0002-0357-1672; Email: jdisch92@gmail.com

Shilpi Arora − *X-Chem Inc., Waltham, Massachusetts 02453, United States*; Email: ssoniarora@gmail.com

Authors

Jennifer M. Duffy − *X-Chem Inc., Waltham, Massachusetts 02453, United States*

Esther C. Y. Lee − *X-Chem Inc., Waltham, Massachusetts 02453, United States*

Diana Gikunju − *X-Chem Inc., Waltham, Massachusetts 02453, United States*

Betty Chan − *X-Chem Inc., Waltham, Massachusetts 02453, United States*

Benjamin Levin − *X-Chem Inc., Waltham, Massachusetts 02453, United States*

Michael I. Monteiro − *X-Chem Inc., Waltham, Massachusetts 02453, United States*

Sarah A. Talcott − *X-Chem Inc., Waltham, Massachusetts 02453, United States*

Anthony C. Lau − *X-Chem Inc., Waltham, Massachusetts 02453, United States*

Fei Zhou − *X-Chem Inc., Waltham, Massachusetts 02453, United States*

Anton Kozhushnyan − *X-Chem Inc., Waltham, Massachusetts 02453, United States*

Neil E. Westlund − *X-Chem Inc., Waltham, Massachusetts 02453, United States*

Patrick B. Mullins − *X-Chem Inc., Waltham, Massachusetts 02453, United States*

Yan Yu − *X-Chem Inc., Waltham, Massachusetts 02453, United States*

Moritz von Rechenberg − *X-Chem Inc., Waltham, Massachusetts 02453, United States*

Junyi Zhang − *X-Chem Inc., Waltham, Massachusetts 02453, United States*

Yelena A. Arnautova − *X-Chem Inc., Waltham, Massachusetts 02453, United States*

Yanbin Liu − *X-Chem Inc., Waltham, Massachusetts 02453, United States*

Ying Zhang − *X-Chem Inc., Waltham, Massachusetts 02453, United States*

Andrew J. McRiner − *X-Chem Inc., Waltham, Massachusetts 02453, United States*
Anthony D. Keefe − *X-Chem Inc., Waltham, Massachusetts 02453, United States*
Anna Kohlmann − *X-Chem Inc., Waltham, Massachusetts 02453, United States*
Matthew A. Clark − *X-Chem Inc., Waltham, Massachusetts 02453, United States*
John W. Cuozzo − *X-Chem Inc., Waltham, Massachusetts 02453, United States;* orcid.org/0000-0002-6229-0395
Christelle Huguet − *X-Chem Inc., Waltham, Massachusetts 02453, United States*

Complete contact information is available at: https://pubs.acs.org/10.1021/acs.jmedchem.1c00127

Author Contributions

J.S.D., E.C.Y.L., J.Z., A.J.M., Y.Z., and M.A.C. contributed to the design of compounds, the establishment of the E3 alkyne toolkit, and evaluation of results; J.M.D. optimized and ran the cell-based viability and degradation assays and other cell-based assays; A.C.L. ran some of the degradation assays; S.A.T. optimized and executed the gene expression analysis. D.G. and B.C. planned and performed the biochemical assays; A.D.K. designed and M.I.M. performed the selections; B.L. and M.v.R. oversaw protein production and performed protein purifications; J.W.C. and C.H. helped plan the biology and *in vivo* experiments; A.K. and Y.A.A. performed the molecular docking; compounds were synthesized by F.Z., A.K., N.E.W., P.B.M., and Y.Y.; Y.L. planned and oversaw the synthesis of the small molecules; A.J.M. and E.C.Y.L. oversaw all outsourced ADME and PK work; J.S.D., E.C.Y.L., A.J.M., and S.A. planned the mouse xenograft efficacy study; S.A. planned and conceived all the biology experiments, oversaw the performance of the outsourced mouse xenograft efficacy study, and was the project lead. All authors helped in writing and reviewing of the manuscript.

Funding

The work included in the manuscript was performed as part of internal drug discovery efforts at X-Chem Inc. No grant support was used.

Notes

The authors declare the following competing financial interest(s): All authors are current or former employees of X-Chem Inc., which conducted the work.

■ ACKNOWLEDGMENTS

Authors would like to thank Marie-Aude Guié and Scott Lindberg for providing scientific database management and Surayya Sana, Masarah Taktak, and Autumn Jetson for compound management. Some of the small molecule synthesis was performed at BioDuro (China).

■ ABBREVIATIONS

ERα, estrogen receptor α; PROTAC, proteolysis targeting chimera; VHL, von Hippel−Lindau E3 ubiquitin ligase; IAP, inhibitor of apoptosis protein; DECL, DNA-encoded chemical library; POI, protein of interest; TGI, tumor growth inhibition; ENRv1, enrichment metric

■ REFERENCES

(1) Bray, F.; Ferlay, J.; Soerjomataram, I.; Siegel, R. L.; Torre, L. A.; Jemal, A. Global cancer statistics 2018: GLOBOCAN estimates of incidence and mortality worldwide for 36 cancers in 185 countries. *CA Cancer J. Clin.* **2018**, *68*, 394−424.
(2) Siersbaek, R.; Kumar, S.; Carroll, J. S. Signaling pathways and steroid receptors modulating estrogen receptor alpha function in breast cancer. *Genes Dev.* **2018**, *32*, 1141−1154.
(3) Waks, A. G.; Winer, E. P. Breast Cancer Treatment: A Review. *JAMA* **2019**, *321*, 288−300.
(4) Lin, X.; Xiang, H.; Luo, G. Targeting estrogen receptor alpha for degradation with PROTACs: A promising approach to overcome endocrine resistance. *Eur. J. Med. Chem.* **2020**, *206*, 112689.
(5) Shagufta; Ahmad, I.; Mathew, S.; Rahman, S. Recent progress in selective estrogen receptor downregulators (SERDs) for the treatment of breast cancer. *RSC Med. Chem.* **2020**, *11*, 438−454.
(6) Gombos, A. Selective oestrogen receptor degraders in breast cancer: a review and perspectives. *Curr. Opin. Oncol.* **2019**, *31*, 424−429.
(7) Gombos, A.; Franzoi, M. A.; Awada, A. Investigational drugs in early stage clinical trials for the treatment of HER2+ breast cancer. *Expert Opin. Invest. Drugs* **2019**, *28*, 617−627.
(8) Nayar, U.; Cohen, O.; Kapstad, C.; Cuoco, M. S.; Waks, A. G.; Wander, S. A.; Painter, C.; Freeman, S.; Persky, N. S.; Marini, L.; Helvie, K.; Oliver, N.; Rozenblatt-Rosen, O.; Ma, C. X.; Regev, A.; Winer, E. P.; Lin, N. U.; Wagle, N. Acquired HER2 mutations in ER(+) metastatic breast cancer confer resistance to estrogen receptor-directed therapies. *Nat. Genet.* **2019**, *51*, 207−216.
(9) Thomas, C.; Gustafsson, J.-A. Estrogen receptor mutations and functional consequences for breast cancer. *Trends Endocrinol. Metab.* **2015**, *26*, 467−476.
(10) Alluri, P. G.; Speers, C.; Chinnaiyan, A. M. Estrogen receptor mutations and their role in breast cancer progression. *Breast Cancer Res.* **2014**, *16*, 494.
(11) Merenbakh-Lamin, K.; Ben-Baruch, N.; Yeheskel, A.; Dvir, A.; Soussan-Gutman, L.; Jeselsohn, R.; Yelensky, R.; Brown, M.; Miller, V. A.; Sarid, D.; Rizel, S.; Klein, B.; Rubinek, T.; Wolf, I. D538G mutation in estrogen receptor-α: A novel mechanism for acquired endocrine resistance in breast cancer. *Cancer Res.* **2013**, *73*, 6856−6864.
(12) Robinson, D. R.; Wu, Y. M.; Vats, P.; Su, F.; Lonigro, R. J.; Cao, X.; Kalyana-Sundaram, S.; Wang, R.; Ning, Y.; Hodges, L.; Gursky, A.; Siddiqui, J.; Tomlins, S. A.; Roychowdhury, S.; Pienta, K. J.; Kim, S. Y.; Roberts, J. S.; Rae, J. M.; Van Poznak, C. H.; Hayes, D. F.; Chugh, R.; Kunju, L. P.; Talpaz, M.; Schott, A. F.; Chinnaiyan, A. M. Activating ESR1 mutations in hormone-resistant metastatic breast cancer. *Nat. Genet.* **2013**, *45*, 1446−1451.
(13) Toy, W.; Weir, H.; Razavi, P.; Lawson, M.; Goeppert, A. U.; Mazzola, A. M.; Smith, A.; Wilson, J.; Morrow, C.; Wong, W. L.; De Stanchina, E.; Carlson, K. E.; Martin, T. S.; Uddin, S.; Li, Z.; Fanning, S.; Katzenellenbogen, J. A.; Greene, G.; Baselga, J.; Chandarlapaty, S. Activating ESR1 Mutations Differentially Affect the Efficacy of ER Antagonists. *Cancer Discovery* **2017**, *7*, 277−287.
(14) Pooh, A. Proof-of-Concept with PROTACs in Prostate Cancer. *Cancer Discovery* **2020**, *10*, 1084.
(15) Gao, H.; Sun, X.; Rao, Y. PROTAC Technology: Opportunities and Challenges. *ACS Med. Chem. Lett.* **2020**, *11*, 237−240.
(16) Sun, X.; Gao, H.; Yang, Y.; He, M.; Wu, Y.; Song, Y.; Tong, Y.; Rao, Y. PROTACs: great opportunities for academia and industry. *Signal Transduction Targeted Ther.* **2019**, *4*, 64.
(17) Li, X.; Song, Y. Proteolysis-targeting chimera (PROTAC) for targeted protein degradation and cancer therapy. *J. Hematol. Oncol.* **2020**, *13*, 50.
(18) Dai, Y.; Yue, N.; Gong, J.; Liu, C.; Li, Q.; Zhou, J.; Huang, W.; Qian, H. Development of cell-permeable peptide-based PROTACs targeting estrogen receptor α. *Eur. J. Med. Chem.* **2020**, *187*, 111967.
(19) Flanagan, J. J.; Neklesa, T. K. Targeting Nuclear Receptors with PROTAC degraders. *Mol. Cell. Endocrinol.* **2019**, *493*, 110452.
(20) Hu, J.; Hu, B.; Wang, M.; Xu, F.; Miao, B.; Yang, C. Y.; Wang, M.; Liu, Z.; Hayes, D. F.; Chinnaswamy, K.; Delproposto, J.; Stuckey, J.; Wang, S. Discovery of ERD-308 as a Highly Potent Proteolysis

Targeting Chimera (PROTAC) Degrader of Estrogen Receptor (ER). *J. Med. Chem.* **2019**, *62*, 1420−1442.
(21) Roberts, B. L.; Ma, Z. X.; Gao, A.; Leisten, E. D.; Yin, D.; Xu, W.; Tang, W. Two-Stage Strategy for Development of Proteolysis Targeting Chimeras and its Application for Estrogen Receptor Degraders. *ACS Chem. Biol.* **2020**, *15*, 1487−1496.
(22) Cyrus, K.; Wehenkel, M.; Choi, E. Y.; Lee, H.; Swanson, H.; Kim, K. B. Jostling for position: optimizing linker location in the design of estrogen receptor-targeting PROTACs. *ChemMedChem* **2010**, *5*, 979−985.
(23) Crew, Andrew P.; Flanagin, John; Gough Sheryl, Maxine; Haskell Royal, J.; Moore Marcia, D.; Qian, Yimin; Taylor Ian, C. A.; Wang, Jing; Xin, C. Methods of treating breast cancer with tetrahydronaphthalene derivatives as Estrogen Receptor Degraders, Patent Application WO/2021/041348. March 4, 2021.
(24) Zorba, A.; Nguyen, C.; Xu, Y.; Starr, J.; Borzilleri, K.; Smith, J.; Zhu, H.; Farley, K. A.; Ding, W.; Schiemer, J.; Feng, X.; Chang, J. S.; Uccello, D. P.; Young, J. A.; Garcia-Irrizary, C. N.; Czabaniuk, L.; Schuff, B.; Oliver, R.; Montgomery, J.; Hayward, M. M.; Coe, J.; Chen, J.; Niosi, M.; Luthra, S.; Shah, J. C.; El-Kattan, A.; Qiu, X.; West, G. M.; Noe, M. C.; Shanmugasundaram, V.; Gilbert, A. M.; Brown, M. F.; Calabrese, M. F. Delineating the role of cooperativity in the design of potent PROTACs for BTK. *Proc. Natl. Acad. Sci. U. S. A.* **2018**, *115*, E7285−E7292.
(25) Clark, M. A.; Acharya, R. A.; Arico-Muendel, C. C.; Belyanskaya, S. L.; Benjamin, D. R.; Carlson, N. R.; Centrella, P. A.; Chiu, C. H.; Creaser, S. P.; Cuozzo, J. W.; Davie, C. P.; Ding, Y.; Franklin, G. J.; Franzen, K. D.; Gefter, M. L.; Hale, S. P.; Hansen, N. J.; Israel, D. I.; Jiang, J.; Kavarana, M. J.; Kelley, M. S.; Kollmann, C. S.; Li, F.; Lind, K.; Mataruse, S.; Medeiros, P. F.; Messer, J. A.; Myers, P.; O'Keefe, H.; Oliff, M. C.; Rise, C. E.; Satz, A. L.; Skinner, S. R.; Svendsen, J. L.; Tang, L.; van Vloten, K.; Wagner, R. W.; Yao, G.; Zhao, B.; Morgan, B. A. Design, synthesis and selection of DNA-encoded small-molecule libraries. *Nat. Chem. Biol.* **2009**, *5*, 647−654.
(26) Harris, P. A.; King, B. W.; Bandyopadhyay, D.; Berger, S. B.; Campobasso, N.; Capriotti, C. A.; Cox, J. A.; Dare, L.; Dong, X.; Finger, J. N.; Grady, L. C.; Hoffman, S. J.; Jeong, J. U.; Kang, J.; Kasparcova, V.; Lakdawala, A. S.; Lehr, R.; McNulty, D. E.; Nagilla, R.; Ouellette, M. T.; Pao, C. S.; Rendina, A. R.; Schaeffer, M. C.; Summerfield, J. D.; Swift, B. A.; Totoritis, R. D.; Ward, P.; Zhang, A.; Zhang, D.; Marquis, R. W.; Bertin, J.; Gough, P. J. DNA-Encoded Library Screening Identifies Benzo[b][1,4]oxazepin-4-ones as Highly Potent and Monoselective Receptor Interacting Protein 1 Kinase Inhibitors. *J. Med. Chem.* **2016**, *59*, 2163−2178.
(27) Belyanskaya, S. L.; Ding, Y.; Callahan, J. F.; Lazaar, A. L.; Israel, D. I. Discovering Drugs with DNA-Encoded Library Technology: From Concept to Clinic with an Inhibitor of Soluble Epoxide Hydrolase. *ChemBioChem* **2017**, *18*, 837−842.
(28) Cuozzo, J. W.; Clark, M. A.; Keefe, A. D.; Kohlmann, A.; Mulvihill, M.; Ni, H.; Renzetti, L. M.; Resnicow, D. I.; Ruebsam, F.; Sigel, E. A.; Thomson, H. A.; Wang, C.; Xie, Z.; Zhang, Y. Novel autotaxin inhibitor for the treatment of idiopathic pulmonary fibrosis: a clinical candidate discovered using DNA-encoded chemistry. *J. Med. Chem.* **2020**, *63*, 7840−7856.
(29) Petersen, L. K.; Christensen, A. B.; Andersen, J.; Folkesson, C. G.; Kristensen, O.; Andersen, C.; Alzu, A.; Slok, F. A.; Blakskjaer, P.; Madsen, D.; Azevedo, C.; Micco, I.; Hansen, N. J. V. Screening of DNA-Encoded Small Molecule Libraries inside a Living Cell. *J. Am. Chem. Soc.* **2021**, *143*, 2751−2756.
(30) McCloskey, K.; Sigel, E. A.; Kearnes, S.; Xue, L.; Tian, X.; Moccia, D.; Gikunju, D.; Bazzaz, S.; Chan, B.; Clark, M. A.; Cuozzo, J. W.; Guie, M. A.; Guilinger, J. P.; Huguet, C.; Hupp, C. D.; Keefe, A. D.; Mulhern, C. J.; Zhang, Y.; Riley, P. Machine Learning on DNA-Encoded Libraries: A New Paradigm for Hit Finding. *J. Med. Chem.* **2020**, *63*, 8857−8866.
(31) Wurz, R. P.; Dellamaggiore, K.; Dou, H.; Javier, N.; Lo, M. C.; McCarter, J. D.; Mohl, D.; Sastri, C.; Lipford, J. R.; Cee, V. J. A "Click Chemistry Platform" for the Rapid Synthesis of Bispecific Molecules for Inducing Protein Degradation. *J. Med. Chem.* **2018**, *61*, 453−461.
(32) Faver, J. C.; Riehle, K.; Lancia, D. R., Jr.; Milbank, J. B. J.; Kollmann, C. S.; Simmons, N.; Yu, Z.; Matzuk, M. M. Quantitative Comparison of Enrichment from DNA-Encoded Chemical Library Selections. *ACS Comb. Sci.* **2019**, *21*, 75−82.
(33) Callis, R.; Rabow, A.; Tonge, M.; Bradbury, R.; Challinor, M.; Roberts, K.; Jones, K.; Walker, G. A Screening Assay Cascade to Identify and Characterize Novel Selective Estrogen Receptor Downregulators (SERDs). *J. Biomol. Screen* **2015**, *20*, 748−759.
(34) Komm, B. S.; Kharode, Y. P.; Bodine, P. V.; Harris, H. A.; Miller, C. P.; Lyttle, C. R. Bazedoxifene acetate: a selective estrogen receptor modulator with improved selectivity. *Endocrinology* **2005**, *146*, 3999−4008.
(35) Miller, C. P.; Collini, M. D.; Tran, B. D.; Harris, H. A.; Kharode, Y. P.; Marzolf, J. T.; Moran, R. A.; Henderson, R. A.; Bender, R. H.; Unwalla, R. J.; Greenberger, L. M.; Yardley, J. P.; Abou-Gharbia, M. A.; Lyttle, C. R.; Komm, B. S. Design, synthesis, and preclinical characterization of novel, highly selective indole estrogens. *J. Med. Chem.* **2001**, *44*, 1654−1657.
(36) Frost, J.; Galdeano, C.; Soares, P.; Gadd, M. S.; Grzes, K. M.; Ellis, L.; Epemolu, O.; Shimamura, S.; Bantscheff, M.; Grandi, P.; Read, K. D.; Cantrell, D. A.; Rocha, S.; Ciulli, A. Potent and selective chemical probe of hypoxic signalling downstream of HIF-α hydroxylation via VHL inhibition. *Nat. Commun.* **2016**, *7*, 13312.
(37) Edmondson, S. D.; Yang, B.; Fallan, C. Proteolysis targeting chimeras (PROTACs) in 'beyond rule-of-five' chemical space: Recent progress and future challenges. *Bioorg. Med. Chem. Lett.* **2019**, *29*, 1555−1564.
(38) Cantrill, C.; Chaturvedi, P.; Rynn, C.; Petrig Schaffland, J.; Walter, I.; Wittwer, M. B. Fundamental aspects of DMPK optimization of targeted protein degraders. *Drug Discovery Today* **2020**, *25*, 969−982.
(39) Naito, M.; Ohoka, N.; Shibata, N.; Tsukumo, Y. Targeted Protein Degradation by Chimeric Small Molecules, PROTACs and SNIPERs. *Front. Chem.* **2019**, *7*, 849.
(40) Sakamoto, K. M.; Kim, K. B.; Kumagai, A.; Mercurio, F.; Crews, C. M.; Deshaies, R. J. Protacs: chimeric molecules that target proteins to the Skp1-Cullin-F box complex for ubiquitination and degradation. *Proc. Natl. Acad. Sci. U. S. A.* **2001**, *98*, 8554−8559.
(41) Mullard, A. First targeted protein degrader hits the clinic. *Nat. Rev. Drug Discovery* **2019**, *18*, 237−239.
(42) Bondeson, D. P.; Mares, A.; Smith, I. E.; Ko, E.; Campos, S.; Miah, A. H.; Mulholland, K. E.; Routly, N.; Buckley, D. L.; Gustafson, J. L.; Zinn, N.; Grandi, P.; Shimamura, S.; Bergamini, G.; Faelth-Savitski, M.; Bantscheff, M.; Cox, C.; Gordon, D. A.; Willard, R. R.; Flanagan, J. J.; Casillas, L. N.; Votta, B. J.; den Besten, W.; Famm, K.; Kruidenier, L.; Carter, P. S.; Harling, J. D.; Churcher, I.; Crews, C. M. Catalytic in vivo protein knockdown by small-molecule PROTACs. *Nat. Chem. Biol.* **2015**, *11*, 611−617.
(43) Churcher, I. Protac-Induced Protein Degradation in Drug Discovery: Breaking the Rules or Just Making New Ones? *J. Med. Chem.* **2018**, *61*, 444−452.
(44) Watt, G. F.; Scott-Stevens, P.; Gaohua, L. Targeted protein degradation in vivo with Proteolysis Targeting Chimeras: Current status and future considerations. *Drug Discovery Today Technol.* **2019**, *31*, 69−80.
(45) Kargbo, R. B. PROTAC-Mediated Degradation of Estrogen Receptor in the Treatment of Cancer. *ACS Med. Chem. Lett.* **2019**, *10*, 1367−1369.
(46) Mares, A.; Miah, A. H.; Smith, I. E. D.; Rackham, M.; Thawani, A. R.; Cryan, J.; Haile, P. A.; Votta, B. J.; Beal, A. M.; Capriotti, C.; Reilly, M. A.; Fisher, D. T.; Zinn, N.; Bantscheff, M.; MacDonald, T. T.; Vossenkamper, A.; Dace, P.; Churcher, I.; Benowitz, A. B.; Watt, G.; Denyer, J.; Scott-Stevens, P.; Harling, J. D. Extended pharmacodynamic responses observed upon PROTAC-mediated degradation of RIPK2. *Commun. Biol.* **2020**, *3*, 140.
(47) den Besten, W.; Lipford, J. R. Prospecting for molecular glues. *Nat. Chem. Biol.* **2020**, *16*, 1157−1158.
(48) Fernández-Montalvan, A. E.; Berger, M.; Kuropka, B.; Koo, S. J.; Badock, V.; Weiske, J.; Puetter, V.; Holton, S. J.; Stockigt, D.; Ter

https://doi.org/10.1021/acs.jmedchem.1c00127
J. Med. Chem. 2021, 64, 5049−5066

Laak, A.; Centrella, P. A.; Clark, M. A.; Dumelin, C. E.; Sigel, E. A.; Soutter, H. H.; Troast, D. M.; Zhang, Y.; Cuozzo, J. W.; Keefe, A. D.; Roche, D.; Rodeschini, V.; Chaikuad, A.; Diaz-Saez, L.; Bennett, J. M.; Fedorov, O.; Huber, K. V. M.; Hubner, J.; Weinmann, H.; Hartung, I. V.; Gorjanacz, M. Isoform-Selective ATAD2 Chemical Probe with Novel Chemical Structure and Unusual Mode of Action. *ACS Chem. Biol.* **2017**, *12*, 2730−2736.

(49) Litovchick, A.; Dumelin, C. E.; Habeshian, S.; Gikunju, D.; Guié, M.-A.; Centrella, P.; Zhang, Y.; Sigel, E. A.; Cuozzo, J. W.; Keefe, A. D.; Clark, M. A. Encoded Library Synthesis Using Chemical Ligation and the Discovery of sEH Inhibitors from a 334-Million Member Library. *Sci. Rep.* **2015**, *5*, 10916.

(50) Livak, K. J.; Schmittgen, T. D. Analysis of relative gene expression data using real-time quantitative PCR and the 2(-Delta Delta C(T)) Method. *Methods* **2001**, *25*, 402−408.

https://doi.org/10.1021/acs.jmedchem.1c00127
J. Med. Chem. 2021, 64, 5049−5066